Table 3b
Genes induced by exemestane treatment in hFOB cells—the osteoblast growth-related genes

	Gene title	Gene symbol	Raw data			Ratio	
			C	D	Ex	D	Ex
K01228	Collagen, type I, alpha 1	**COL1A1**	2797.2	3240.9	3058.5	1.2	1.1
BE221212	Collagen, type I, alpha 1	**COL1A1**	2741.1	3048.3	3052.2	1.1	1.1
AI743621	Collagen, type I, alpha 1	**COL1A1**	228.0	241.6	242.5	1.1	1.1
AA788711	Collagen, type I, alpha 2	COL1A2	2250.6	2474.3	2375.4	1.1	1.1
NM_000089	Collagen, type I, alpha 2	COL1A2	1749.1	1848.7	1787.6	1.1	1.0
M60485	Fibroblast growth factor receptor 1	FGFR1	178.9	185.7	198.6	1.0	1.1
BE467261	Fibroblast growth factor receptor 1	FGFR1	165.4	208.6	189.7	1.3	1.1
M63889	Fibroblast growth factor receptor 1	FGFR1	119.3	111.6	140.5	0.9	1.2
NM_023110	Fibroblast growth factor receptor 1	FGFR1	60.5	84.0	70.2	1.4	1.2
AU145411	Fibroblast growth factor receptor 1	FGFR1	29.2	44.1	37.5	1.5	1.3
AI359368	Fibroblast growth factor receptor 3	FGFR3	41.4	65.5	58.7	1.6	1.4
NM_001552	Insulin-like growth factor binding protein 4	IGFBP4	809.1	1027.5	1040.4	1.3	1.3
AL353944	Runt-related transcription factor 2	**RUNX2**	192.9	226.3	216.3	1.2	1.1
AU146891	SMAD, mothers against DPP homolog 1 (*Drosophila*)	**SMAD1**	161.2	195.6	204.6	1.2	1.3
NM_005901	SMAD, mothers against DPP homolog 2 (*Drosophila*)	SMAD2	100.3	108.2	113.7	1.1	1.1
NM_005902	SMAD, mothers against DPP homolog 3 (*Drosophila*)	SMAD3	110.2	106.5	127.7	1.0	1.2
BF526175	SMAD, mothers against DPP homolog 5 (*Drosophila*)	**SMAD5**	361.0	488.3	514.2	1.4	1.4
AI478523	SMAD, mothers against DPP homolog 5 (*Drosophila*)	SMAD5	300.7	384.9	346.9	1.3	1.2
AF010601	SMAD, mothers against DPP homolog 5 (*Drosophila*)	SMAD5	79.2	99.7	87.6	1.3	1.1
AY014180	SMAD-specific E3 ubiquitin protein ligase 2	SMURF2	804.2	844.7	851.8	1.1	1.1
AU157259	SMAD-specific E3 ubiquitin protein ligase 2	SMURF2	77.1	81.5	86.3	1.1	1.1
AL575922	Secreted protein, acidic, cysteine-rich (osteonectin)	**SPARC**	1702.1	1935.5	1925.8	1.1	1.1
BF508662	Sprouty homolog 1, antagonist of FGF signaling (*Drosophila*)	SPRY1	31.9	46.3	45.4	1.5	1.4
NM_014886	TGF beta-inducible nuclear protein 1	TINP1	1185.7	1259.5	1241.1	1.1	1.0

C, vehicle control; D, 5α-dihydrotestosterone; Ex, exemestane. Genes that performed quantitative RT-PCR were described in bold style.

steroidal aromatase inhibitor, has been therefore attributed to its actions through AR in osteoblasts. Systemic androgenic effects such as hypertricosis, hair loss, hoarseness, and acne have been reported only in 4% [6] of the patients treated with EXE (25 mg/day) and the frequency of these effects increases to approximately 10% in those treated with higher dose 200 mg/day of EXE [6]. This finding suggests that the patients treated with EXE are under relatively weak systemic androgenic effects. Androgen sensitivity has been well-known to be subject to great individual variation caused by AR gene CAG polymorphism in women as well as men [29,30]. Therefore, this 5 to 10% of the patients who manifested clinical androgenic effects by EXE treatment may be individuals associated with relatively enhanced androgenic sensitivity. Replacement therapy with TST is generally effective at restoring bone in hypogonadal men [31]. In female-to-male, genetic female transsexual subjects, high-dose TST therapy generally increased BMD at the femoral neck, despite decrement of E2 to postmenopausal levels [32,33]. Therefore, androgens may play an important role in bone protection in women as well as men.

The results of cell proliferation assay demonstrated that the cell number of MG-63 was increased by both E2 and DHT treatments, but the dose of DHT was relatively higher than that in two other cells. MG-63 expressed higher levels of ERα/β mRNA, but the level of AR mRNA was lower than that in both Saos-2 and hFOB. Both cell proliferation and ALP activity of MG-63 could not be stimulated by EXE treatment. Molecular mechanisms of androgen actions on osteoblasts have remained largely unknown. Androgen is well-known to stimulate osteoblast proliferation [34] and differentiation [35]. For instance, osteoprotegerin mRNA was increased by TST as well as DHT treatments in mouse 3T3-E1 cells [36].

AR and ERβ but not ERα are predominantly detected in osteoblasts located on human cancellous bone using immunohistochemical analysis [37]. Therefore, hFOB examined in this study is considered to maintain relatively native status of sex steroids pathways in human osteoblasts. Therefore, we employed hFOB for further examination of EXE effects on osteoblast gene expression pattern using microarray analysis. In this study, we demonstrated that the genes MYBL2 [38], OSTM1 [39], HOXD11 [40], ADCYAP1R1 [41], and GPC2 [42] were target genes of EXE alone or both EXE and DHT in hFOB using microarray/PCR analysis. These genes were demonstrated to be involved in regulation of cell cycle, differentiation, and transcription. In EXE or DHT treatment in hFOB and Saos-2, in which cells proliferations were stimulated, an increased expression of HOXD11 gene was detected. The product of the mouse Hoxd11 gene was reported to play a role in forelimb morphogenesis [40,43]. Therefore, these finding suggest that osteoblast cell proliferation stimulated by EXE treatment may depend on HOXD11 gene expression through AR. In this study, the cell proliferation of MG-63, which expressed relatively low level of AR, was not stimulated by EXE. In addition, HOXD11 gene expression was not up-regulated by EXE treatment in MG-63 cells. These results were also consist with the protective effects of EXE through potential androgen-HOXD11 pathway in osteoblast cells. In this study, we also examined the effects of EXE and DHT on osteoblast growth-related genes using micro-

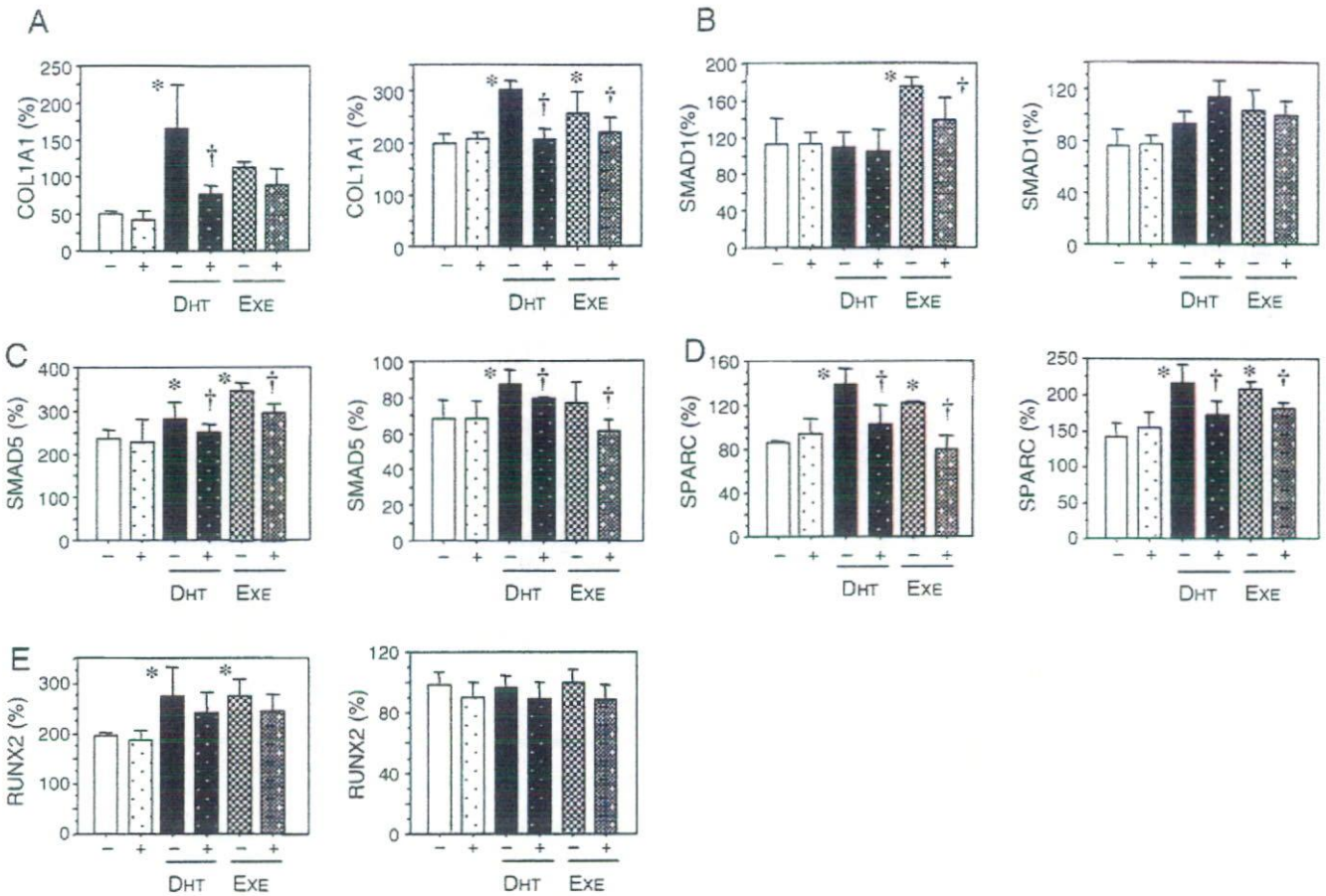

Fig. 7. Expression levels of osteoblast growth-related genes in hFOB (left) and Saos-2 (right). DHT: 10^{-8} M 5α-dihydrotestosterone, EXE: 10^{-7} M Exemestane, with (+) or without (−) hydroxyflutamide, $p<0.05$ vs. control (*) or without hydroxyflutamide (†).

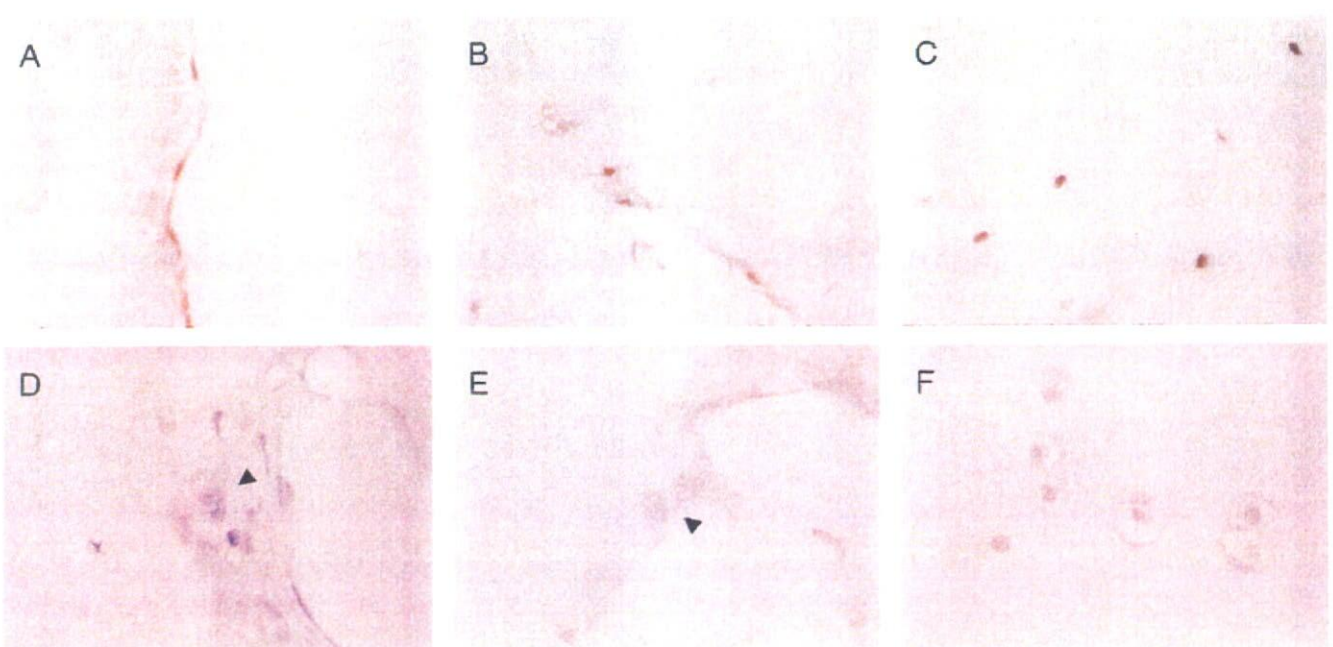

Fig. 8. Immunohistochemistry of androgen receptor in human bone tissues. Immunoreactivity of androgen receptor was detected in nuclei of osteoblasts/liner cells (A, B) but not in osteoclasts (D, E; arrowheads). Immunoreactivity of androgen receptor was also detected in nuclei of osteocytes (C) and condrocytes (F).

array analysis and following quantitative RT-PCR. COL1A1, SMAD5, and SPARC (osteonectine) were up-regulated by EXE and/or DHT treatments in both hFOB and Saos-2 cells. EXE or DHT treatments in both hFOB and Saos-2 also resulted in increased ALP activity. There have been, however, no studies reported on whether these genes are primary or secondary androgen responsive genes in osteoblasts. The AR-specific antagonist, OHF demonstrated no inhibitory effects on RUNX2 expression increased by EXE or DHT treatment in hFOB cells. In addition, hFOB cell growth induced by high dose of EXE treatment was not completely inhibited by OHF treatment. These results all suggest that EXE also may stimulate hFOB cell proliferation through both AR dependent and independent pathways. From our data of steroid production in hFOB, EXE may have an additional androgenic effect through increased TST levels in conjunction with inhibition of aromatization in hFOB cells. However, it awaits further investigations for clarification.

In normal bone remodeling, bone formation by osteoblasts follows bone resorption by osteoclasts and occurs in a precise and quantitative manner (coupling). In this coupling between bone formation and resorption, a coupling factor that induces bone formation is considered to be released during osteoclastic bone resorption [44]. This study has focused on the specific effects on osteoblast cells. However, it is true that there were significant increases in both serum bone formation and resorption markers in postmenopausal women administered with EXE for 2 years [26]. Osteoclasts, which are responsible for bone resorption, are target cells for many anti-osteoporosis therapeutic agents such as bisphosphonate of postmenopausal women [45]. However, it is unclear whether EXE acts on osteoclast directly. Chen et al. [46] reported that testosterone inhibited osteoclast formation stimulated by parathyroid hormone through the AR but not through the production of intrinsic estrogen using primary mouse osteoclast cells. In both human and rodent bone tissues, AR is expressed in both osteoblasts and osteocytes [47,48]. However, AR is detected in osteoclasts of rodent but not in human cells [31,47,48]. Therefore, in humans, androgens are considered to exert their effects on bone through osteoblasts. EXE may therefore exert its possible androgenic effects on human bone through osteoblasts but not osteoclasts. Results of our present study also suggest the possible roles of EXE on osteoblast cells through AR independent manner. Results of clinical studies suggest that the combination therapy of AI and COX-2 inhibitors could provide more effective aromatase inhibition than single therapy in hormone-sensitive postmenopausal breast cancer [49]. Bone resorption induced by IL-1 and IL-6 was also reported to occur via stimulation of COX-2 dependent PGE_2 production in osteoblasts *in vitro* [50]. Therefore, further investigations are required to clarify the effects of AI including EXE on human bone tissues.

In summary, this study using osteoblast and osteoblast-like cell lines suggested the potential protective effect of steroidal AI, EXE on osteoblasts occurred through both AR dependent and independent pathways. HOXD11 gene known as bone morphogenesis factor and osteoblast growth-related genes were induced by EXE treatment as well as DHT treatment in both hFOB and Saos-2. Damages of bone tissues by estrogen depletion caused by AI administration are considered unavoidable but the selection of potential hormone therapies which could minimize the damages or injuries of bone tissues is considered important.

Acknowledgments

We appreciate Dr. Shin-ichi Hayashi (Divisions of Molecular Medical Technology, Tohoku University School of Medicine) for critical comments. We also appreciate Ms. Chika Tazawa, Ms. Toshie Suzuki, Ms. Miki Mori and Mr. Katsuhiko Ono (Department of Pathology, Tohoku University School of Medicine) for skillful technical assistances. This research was supported by Grant-in-aid for Health and Labor Sciences Research Grant on Risk of Chemical Substances (H16-Kagaku-002) from Ministry of Health, Labor, and Welfare, Japan and Kanzawa Medical Research Foundation, Nagano, Japan.

References

[1] Rogers J. Estrogens in the menopause and postmenopause. N Engl J Med 1969;280:364–7.
[2] Wingate L. The epidemiology of osteoporosis. J Med 1984;15:245–66.
[3] Felson DT, Zhang Y, Hannan MT, Kiel DP, Wilson PW, Anderson JJ. The effect of postmenopausal estrogen therapy on bone density in elderly women. N Engl J Med 1993;329:1141–6.
[4] Lester L, Coleman R. Bone loss and the aromatase inhibitors. Br J Cancer 2005;93:S16–22.
[5] Miller WR, Dixon JM. Antiaromatase agents: preclinical data and neoadjuvant therapy. Clin Breast Cancer 2000;1:S9–S14.
[6] Lønning PE, Paridaens R, Thurlimann B, Piscitelli G, di Salle E. Exemestane experience in breast cancer treatment. J Steroid Biochem Mol Biol 1997;61:151–5.
[7] Center for Drug Evaluation and Research Application Number NDA 20753 (Exemestane) Medical Review. Food and Drug Administration, 1999.
[8] Goss PE, Qi S, Josse RG, Pritzker KPH, Mendes M, Hu H, et al. The steroidal Aromatase inhibitor exemestane prevent bone loss in ovariectomized rats. Bone 2004;34:384–92.
[9] Goss PE, Qi S, Cheung AM, Hu H, Mendes M, Pritzker KPH. Effects of steroidal aromatase inhibitor exemestane and the nonsteroidal aromatase inhibitor letrozole on bone and lipid metabolism in the ovariectomized rats. Clin Cancer Res 2004;10:5717–23.
[10] Sasano H, Uzuki M, Sawai T, Nagura H, Matsunaga G, Kashimoto O, et al. Aromatase in human bone tissue. J Bone Miner Res 1997;12:1416–23.
[11] Schweikert HU, Wolf L, Romalo G. Oestrogen formation from Androstendione in human bone. Clin Endocrinol 1995;43:37–42.
[12] Purohit A, Flanagan AM, Reed MJ. Estrogen synthesis by osteoblast cell lines. Endocrinology 1992;131:2027–9.
[13] Tanaka S, Haji M, Nishi Y, Yanase T, Takayanagi R, Nawata H. Aromatase activity in human osteoblast-like osteosarcoma cell. Calcif Tissue Int 1993;52:107–9.
[14] Recanatini M, Bisi A, Cavalli A, Belluti F, Gobbi S, Rampa A, et al. A new class of nonsteroidal aromatase inhibitors: design and synthesis of chromone and xanthone derivatives and inhibition of the P450 enzymes aromatase and 17 alpha-hydroxylase/C17,20-lyase. J Med Chem 2001;44:672–80.
[15] Linkhart TA, Mohan S, Baylink DJ. Growth factors for bone growth and repair: IGF, TGF beta and BMP. Bone 1996;19:1S–12S.
[16] Harris SA, Enger RJ, Riggs BL, Spelsberg TC. Development and characterization of a conditionally immortalized human fetal osteoblastic cell line. J Bone Miner Res 1995;10:178–86.
[17] Suzuki T, Darnel AD, Akahira JI, Ariga N, Ogawa S, Kaneko C, et al. 5alpha-reductases in human breast carcinoma: possible modulator of in situ androgenic actions. J Clin Endocrinol Metab 2001;86:2250–7.

[18] Miki Y, Suzuki T, Tazawa C, Ishizuka M, Semba S, Gorai I, et al. Analysis of gene expression induced by diethylstilbestrol (DES) in human primitive Müllerian duct cells using microarray. Cancer Lett 2005;220:197–210.
[19] Yamamoto M, Takahashi Y, Tabata Y. Controlled release by biodegradable hydrogels enhances the ectopic bone formation of bone morphogenetic protein. Biomaterials 2003;24:4375–83.
[20] Kanno J, Aisaki K, Igarashi K, Nakatsu N, Ono A, Kodama Y, et al. "Per cell" normalization method for mRNA measurement by quantitative PCR and microarrays. BMC Genomics 2006;29:64.
[21] Eisen MB, Spellman PT, Brown PO, Bostein D. Cluster analysis and display of genome-wide expression patterns. Proc Natl Acad Sci U S A 1998;95:14863–8.
[22] Miki Y, Nakata T, Suzuki T, Darnel AD, Moriya T, Kaneko C, et al. Systemic distribution of steroid sulfatase and estrogen sulfotransferase in human adult and fetal tissues. J Clin Endcrinol Metab 2002;87:5760–8.
[23] Ishizuka M, Hatori M, Suzuki T, Miki Y, Darnel AD, Tazawa C, et al. Sex steroid receptors in rheumatoid arthritis. Clin Sci (Lond) 2004;106: 293–300.
[24] Rodan GA, Noda M. Gene expression in osteoblastic cells. Crit Rev Eukaryot Gene Expr 1991;1:85–98.
[25] Ito Y, Miyazono K. RUNX transcription factors as key role of TGF-β superfamily signaling. Curr Opin Genet Dev 2003;13:43–7.
[26] Lønning PE, Geisler J, Krag LE, Erikstein B, Bremnes Y, Hagen AI, et al. Effects of exemestane administered for 2 years versus placebo on bone mineral density, bone biomarkers, and plasma lipids in patients with surgically respected early breast cancer. J Clin Oncol 2005;23:4847–9.
[27] Coombes RC, Hall E, Gibson LJ, Paridaens R, Jassem J, Delozier T, et al. Intergroup Exemestane Study. A randomized trial of exemestane after two to three years of tamoxifen therapy in postmenopausal women with primary breast cancer. N Engl J Med 2004;350:1081–92.
[28] Coleman RE, Banks LM, Girgis SI, Vrdoljak E, Fox J, Porter LS, et al. Skeletal effect of exemestane in the Intergroup Exemestane Study (IES)—2 years bone mineral density (BMD) and bone biomarker data. Breast Cancer Res Treat 2005;94:S233.
[29] Vottero A, Stratalis CA, Ghizzoni L, Longui CA, Karl M, Chrousos GP. Androgen receptor-mediated hypersensitivity to androgen in women with nonhyperandrogenic hirsutism: skewing of X-chromosome inactivation. J Clin Endocrinol Metab 1999;84:1091–5.
[30] Brum IS, Spritzer PM, Paris F, Maturana MA, Audran F, Sultan C. Association between androgen receptor gene CAG repeat polymorphism and plasma testosterone levels in postmenopausal women. J Soc Gynecol Investig 2005;12:135–41.
[31] Vanderschueren D, Vandenput L, Boonen S, Lindberg MK, Bouillon R, Ohlsson C. Androgens and bone. Endocr Rev 2004;25:389–425.
[32] Turner A, Chen T, Barber T, Malabanan A, Holick M, Tangpricha V. Testosterone increases bone mineral density in female-to-male transsexuals: a case series of 15 subjects. Clin Endocrinol (Oxf) 2004;61:560–6.
[33] Ruetsche AG, Kneubuehl R, Birkhaeuser MH, Lippuner K. Cortical and trabecular bone mineral density in transsexuals after long-term cross-sex hormonal treatment: a cross-sectional study. Osteoporos Int 2005;16: 791–98.
[34] Kasperk CH, Wergedal JE, Farley JR, Linkhart TA, Turner RT, Baylink DJ. Androgens directly stimulate proliferation of bone cells in vitro. Endocrinology 1989;124:1576–8.
[35] Kasperk C, Fitzsimmons R, Strong D, Mohan S, Jennings J, Wergedal J, et al. Studies of the mechanism by which androgens enhance mitogenesis and differentiation in bone cells. J Clin Endocrinol Metab 1990;71:1322–9.
[36] Chen Q, Kaji H, Kanatani M, Sugimoto T, Chihara K. Testosterone increases osteoprotegerin mRNA expression in mouse osteoblast cells. Horm Metab Res 2004;36:674–8.
[37] Bord S, Horner A, Beavan S, Compston J. Estrogen receptors alpha and beta are differentially expressed in developing human bone. J Clin Endocrinol Metab 2001;86:2309–14.
[38] Sala A, Watson R. B-Myb protein in cellular proliferation, transcription control, and cancer: latest developments. J Cell Physiol 1999;179:245–50.
[39] Chalhoub N, Benachenhou N, Rajapurohitam V, Pata M, Ferron M, Frattini A, et al. Grey-lethal mutation induces severe malignant autosomal recessive osteopetrosis in mouse and human. Nat Med 2003;9:399–406.
[40] Boulet AM, Capecchi MR. Multiple roles of Hoxa11 and Hoxd11 in the formation of the mammalian forelimb zeugopod. Development 2004; 131:299–309.
[41] Lundberg P, Lundgren I, Mukohyama H, Lehenkari PP, Horton MA, Lerner UH. Vasoactive intestinal peptide (VIP)/pituitary adenylate cyclase-activating peptide receptor subtypes in mouse calvarial osteoblasts: presence of VIP-2 receptors and differentiation-induced expression of VIP-1 receptors. Endocrinology 2001;142:339–47.
[42] Gutierrez J, Osses N, Brandan E. Changes in secreted and cell associated proteoglycan synthesis during conversion of myoblasts to osteoblasts in response to bone morphogenetic protein-2: role of decorin in cell response to BMP-2. J Cell Physiol 2006;206:58–67.
[43] Omi M, Fisher M, Maihle NJ, Dealy CN. Studies on epidermal growth factor receptor signaling in vertebrate limb patterning. Dev Dyn 2005;233:288–300.
[44] Rodan GA, Raisz LG, Bilezikian JP. Pathophysiology of osteoporosis. . (chapter 73)In: Bilezikian JP, Raisz LG, Rodan GA, editors. Principles of bone biology, 2nd ed., vol. 1. NY, USA: Academic Press, A division of Harcourt, Inc.; 2002. p. 1275–90.
[45] Kellinsalmi M, Monkkonen H, Monkkonen J, Leskela HV, Parikka V, Hamalainen M, et al. In vitro comparison of clodronate, pamidronate and zoledronic acid effects on rat osteoclasts and human stem cell-derived osteoblasts. Basic Clin Pharmacol Toxicol 2005;97:382–91.
[46] Chen Q, Kaji H, Sugimoto T, Chihara K. Testosterone inhibits osteoclast formation stimulated by parathyroid hormone through androgen receptor. FEBS Lett 2001;491:91–3.
[47] Abu EO, Horner A, Kusec V, Triffitt JT, Compston JE. The localization of androgen receptors in human bone. J Clin Endocrinol Metab 1997; 82:3493–7.
[48] Wiren KM, Orwoll ES. Androgens: receptor expression and steroid action in bone. . (chapter 43)In: Bilezikian JP, Raisz LG, Rodan GA, editors. Principles of bone biology, 2nd ed., vol. 1. NY, USA: Academic Press, A division of Harcourt, Inc.; 2002. p. 757–72.
[49] Chow LW, Wong JL, Toi M. Celecoxib anti-aromatase neoadjuvant (CAAN) trial for locally advanced breast cancer: preliminary report. J Steroid Biochem Mol Biol 2003;86:443–7.
[50] Sato T, Morita I, Sakaguchi K, Nakahama KI, Smith WL, Dewitt DL, et al. Involvement of prostaglandin endoperoxide H synthase-2 in osteoclast-like cell formation induced by interleukin-1 beta. J Bone Miner Res 1996;11:392–400.

WILEY InterScience®
DISCOVER SOMETHING GREAT

Hypothalamus Region-Specific Global Gene Expression Profiling in Early Stages of Central Endocrine Disruption in Rat Neonates Injected with Estradiol Benzoate or Flutamide

Makoto Shibutani,[1] Kyoung-Youl Lee,[1]* Katsuhide Igarashi,[2] Gye-Hyeong Woo,[1] Kaoru Inoue,[1] Tetsuji Nishimura,[3] Masao Hirose[1]

[1] Division of Pathology, National Institute of Health Sciences, Setagaya-ku, Tokyo 158-8501, Japan

[2] Division of Molecular Toxicology, National Institute of Health Sciences, Setagaya-ku, Tokyo 158-8501, Japan

[3] Division of Environmental Chemistry, National Institute of Health Sciences, Setagaya-ku, Tokyo 158-8501, Japan

Received 3 February 2006; revised 8 September 2006; accepted 14 September 2006

ABSTRACT: To identify genes linked to early stages of disruption of brain sexual differentiation, hypothalamic region-specific microarray analyses were performed using a microdissection technique with neonatal rats exposed to endocrine-acting drugs. To validate the methodology, the expression fidelity of microarrays was first examined with two-round amplified antisense RNAs (aRNAs) from methacarn-fixed paraffin-embedded tissue (PET) in comparison with expression in unfixed frozen tissue (UFT). Decline of expression fidelity when compared with the 1×-amplified aRNAs from UFTs was found as a result of the preferential amplification of the 3′ side of mRNAs in the second round *in vitro* transcription. However, expression patterns for the 2×-amplified aRNAs were mostly identical between methacarn-fixed PET and UFT, suggesting no obvious influence of methacarn fixation and subsequent paraffin embedding on expression levels. Next, in the main experiment, neonatal rats at birth were treated subcutaneously either with estradiol benzoate (EB; 10 μg/pup) or flutamide (FA; 250 μg/pup), and medial preoptic area (MPOA)-specific microarray analysis was performed 24 h later using 2×-amplified aRNAs from methacarn-fixed PET. Numbers of genes showing constitutively high expression in the MPOA predominated in males, implying a link with male-type growth supported by perinatal testosterone. Around 60% of genes showing sex differences in expression demonstrated altered levels after EB treatment in females, suggesting an involvement of genes necessary for brain sexual differentiation. When compared with EB, FA affected a rather small number of genes, but fluctuation was mostly observed in females, as with EB. Moreover, many selected genes common to EB and FA showed down-regulation in females with both drugs, suggesting a common mechanism for endocrine center disruption in females, at least at early stages of post-natal development. © 2007 Wiley Periodicals, Inc. Develop Neurobiol 67: 253–269, 2007

Keywords: brain sexual differentiation; microarray; estradiol benzoate; flutamide; microdissection

INTRODUCTION

Sex steroids play important roles in sexual differentiation of the mammalian brain (McEwen and Alves, 1999). In the rat, there is a critical period beginning

*Present address: Toxicological Research Team, Occupational Safety and Health Research Institute, 104-8, Munji-Dong, Yuseong-Gu, Daejeon, 305-380, Korea.

Correspondence to: M. Shibutani (shibutan@nihs.go.jp).

Contract grant sponsors: Ministry of the Environment, Ministry of Health, Labor and Welfare of Japan.

© 2007 Wiley Periodicals, Inc.

Published online 3 January 2007 in Wiley InterScience (www.interscience.wiley.com).
DOI 10.1002/dneu.20349

at the last week of gestation and terminating in few days after birth, during which circulating testosterone secreted from the fetal and neonatal testes masculinizes the brain in males (Rhees et al., 1990a,b), the hormone being metabolized to estradiol by the enzyme aromatase to trigger brain sexual differentiation. Steroid-mediated processes during this period, including alterations in neuronal plasticity, myelination, and cell death, are the basis of sexual dimorphism in the structure and function of the adult brain (Matsumoto et al., 2000). For example, the medial preoptic area (MPOA) in the hypothalamus that is believed to mediate sexually dimorphic behavior in adult life (Meisel and Sachs, 1994; Numan, 1994) contains a highly cellular region, the sexually dimorphic nucleus of preoptic area (SDN-POA), that has an approximately 10 times larger volume in males than in females (Meredith et al., 2001). Inhibitory effects of steroids against the normal apoptosis that proceeds in the female SDN-POA during the critical period have been suggested to be responsible for the large size in males (Arai et al., 1996; Davis et al., 1996).

Sex steroids with their receptors are powerful regulators of gene transcription, and changes in the hormonal milieu during development can trigger reproductive dysfunction in later life by affecting molecular cascades responsible for sexual differentiation (McEwen and Alves, 1999). For instance, both α and β estrogen receptors (ERs) are strongly expressed in the hypothalamus during neonatal development, showing region-specific distributions (Orikasa et al., 2002), and neonatal hormonal manipulations can affect their expression levels and/or locations (Tena-Sempere et al., 2001; Orikasa et al., 2002), resulting in organizational changes in the brain structure and reproductive function in later life (Nagao et al., 1999; Tsukahara et al., 2003).

To elucidate mechanisms underlying disruption of brain sexual differentiation, gene screening applying global gene expression profiling in target brain region(s) is an effective approach. We recently established multipurpose genetic analysis methods with paraffin-embedded tissues (PETs) utilizing methacarn as a novel fixation tool, in combination with laser microbeam microdissection (Shibutani et al., 2000; Shibutani and Uneyama, 2002; Uneyama et al., 2002). With this system, we could achieve high performance regarding quantitative expression analysis of mRNAs using real-time RT-PCR, close to that with unfixed frozen tissue (UFT) (Takagi et al., 2004).

In the present study, we focused on region-specific gene expression analysis utilizing microarrays to identify genes linked with disruption of brain sexual differentiation in rats. With limited tissue samples, such as those collected by microdissection, multiround amplification of mRNAs is necessary to obtain sufficient quantities of antisense RNAs (aRNAs) applicable for microarray analysis, and therefore, we first performed validation experiments using methacarn-fixed liver PETs to determine fidelity of expression profiles with 2× *in vitro* transcribed aRNAs in comparison with 1×- or 2×-amplified examples from UFTs. After confirmation of the efficacy of the methods, we then analyzed gene expression profiles in the neonatal MPOA in terms of sex differences and acute responses to neonatally injected estradiol benzoate (EB), a potent analog of endogenous estrogen, or flutamide (FA), a non-steroidal anti-androgen.

METHODS

Chemicals and Animals

Estradiol benzoate (EB; CAS# 50-50-0) and flutamide (FA; CAS# 13311-84-7) were purchased from Sigma (St. Louis, MO), sodium phenobarbital (PB; CAS# 57-30-7) from Wako Pure Chemical Industries (Osaka, Japan) and CD$^{®}$(SD)IGS rats from Charles River Japan (Kanagawa, Japan). For the preliminary validation study regarding expression fidelity with microarrays using methacarn-fixed PET, one 7-week-old male rat was used, and for gene expression profiling in the early stage of disruption of brain sexual differentiation, six pregnant rats at gestational Day 3 (the day when vaginal plugs were observed was designated as GD 0). The animals were housed individually in polycarbonate cages (SK-Clean, 41.5 × 26 × 17.5 cm in size; CLEA Japan, Tokyo) with wood bedding (Soft Chip; Sankyo Lab Service, Tokyo, Japan), maintained in an air-conditioned animal room (temperature: 24°C ± 1°C, relative humidity: 55% ± 5%) with a 12-h light–dark cycle, and allowed *ad libitum* access to feed and tap water. For the rat in the preliminary validation study, CRF-1, a standard rodent diet, purchased from Oriental Yeast Co. (Tokyo, Japan), was used as the basal diet. For pregnant animals, soy-free diet (Oriental Yeast Co.) was used as a basal diet to remove possible interaction of phytoestrogens included in the regular soy-containing diet with the action of EB or FA. The formulation of the soy-free diet as well as the dietary concentrations of estrogens and phytoestrogens were as described earlier (Masutomi et al., 2003). Essentially, concentrations of phytoestrogens except for coumestrol, detected at 0.3 mg/100 g diet, were lower than the detection limit (0.05 mg/100 g diet).

Experimental Design

In the preliminary validation study, the rat received PB intraperitoneally at 80 mg/kg, once daily for three days. The dose was selected according to the PB-specific enzyme

induction protocol described by Kocarek et al. (1998). One day after the last injection, the animal was killed by exsanguination from the abdominal aorta under ether anesthesia, and the liver was removed and trimmed to make tissue blocks sized 5 × 5 × 3 mm.

For gene expression profiling in the early stage of disruption of brain sexual differentiation, offspring of two dams each were injected subcutaneously either with EB, FA, or vehicle at postnatal day (PND) 1 (the day of delivery) within 3–6 h after completion of delivery. The dose level of EB was set as 10 μg/pup, shown in our laboratory, to induce typical estrogenic effects on sexual development and the endocrine/reproductive system at the adult stage in both sexes, including reduction of the SDN volume in males (Shibutani et al., 2005). For FA, 250 μg/pup was selected on the basis of earlier study finding of retardation of male reproductive development with repeated injections of this dose (Rivas et al., 2002). Each chemical was dissolved in sesame oil to achieve a total injection volume of 20 μL. Vehicle control animals were injected with 20 μL of sesame oil. Twenty-four hours after the injection (PND 2), offspring including vehicle control pups were killed by decapitation for removal of brains.

The animal protocols were reviewed and approved by the Animal Care and Use Committee of the National Institute of Health Sciences, Japan.

Preparation of Tissue Specimens and Microdissection

Liver tissues of the rat treated with PB were either quick frozen in ethanol–dry ice after embedding in Tissue-Tek 4583 OCT compound (Sakura Finetek Japan, Tokyo, Japan), or immersed in methacarn for tissue fixation. For this purpose, methacarn solution consisting of 60% (vol/vol) absolute methanol, 30% chloroform, and 10% glacial acetic acid was freshly prepared and stored at 4°C (Shibutani et al., 2000; Shibutani and Uneyama, 2002; Takagi et al., 2004), before fixation for 2 h at 4°C. Fixed tissue samples were then dehydrated three times for 1 h in fresh 99.5% ethanol at 4°C, immersed in xylene once for 1 h and then three times for 30 min at room temperature, and immersed in hot paraffin (60°C) four times for 1 h, for a total of 4 h. Both UFTs (n = 3) and methacarn-fixed PETs (n = 3) were sectioned at 10 μm and 20 sections per block were stored in 1.5 mL tubes at −80°C until RNA extraction.

For MPOA-specific microarray analysis, whole brains of rat pups were subjected to methacarn fixation (n = 3/sex/group). Before embedding, coronal brain slices including the hypothalamus were trimmed. Microdissection of the MPOA was performed based on the method described earlier (Takagi et al., 2004). After paraffin embedding, 6-μm-thick sections between three 18-μm-thick sections were prepared. The 18-μm sections were mounted onto PEN-foil film (Leica Microsystems, Tokyo, Japan) overlaid on glass slides, dried in an incubator overnight at 37°C, deparaffinized with xylene three times each for 3 min, placed in 99.5% ethanol for 1 min, and then air-dried. The localization of the SDN-POA, identified as an intensely stained cellular region, was determined by microscopic observation of the 6-μm-thick sections stained with hematoxylin and eosin (HE) (as shown in Fig. 1), and bilateral portions of the MPOA (500 × 300 μm) containing SDN-POA were microdissected from the adjacent unstained 18-μm-thick sections using PALM Robot-MicroBeam equipment (Carl Zeiss Co., Tokyo, Japan). In both sexes, 10–12 sections from one animal were used for microdissection, and the microdissected samples were stored in one 1.5 mL sample tube at −80°C until extraction of total RNA.

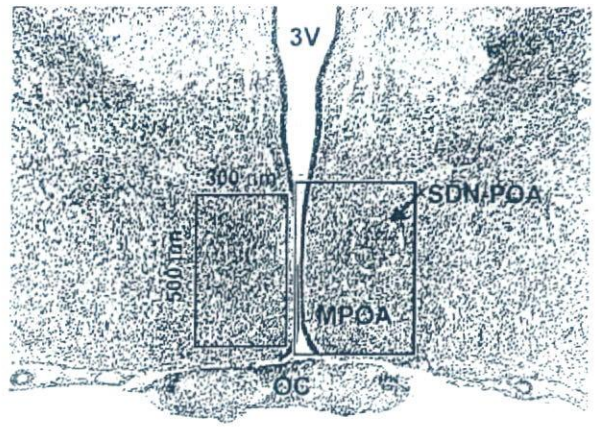

Figure 1 Overview of the hypothalamic MPOA at PND 2. Bilateral portions of MPOA as shown in the left boxed area were microdissected from sections of methacarn-fixed paraffin-embedded brain slices for gene expression analysis. The right boxed area is the anatomical location for immunohistochemical observation of protein signals shown in Table 6 and Fig. 6 (3V, third ventricle; SDN-POA, sexually dimorphic nucleus of the preoptic area; MPOA, medial preoptic area; OC, optic chiasm).

RNA Isolation, Amplification, and Microarray Analysis

Total RNAs from liver sections of UFTs and methacarn-fixed PETs were extracted with RNeasy® Mini (QIAGEN, Hilden, Germany) according to the manufacturer's protocol, with the final elution volume set at 30 μL. Contaminating genomic DNA was digested with DNase I (Ambion, Austin, TX) at the end of the extraction. Total RNAs from microdissected MPOAs were extracted using an RNAquous®-Micro RNA isolation kit (Ambion), eluted twice with a total volume of 14 μL, and then treated with DNase according to the manufacturer's protocol.

For quantitation of RNA yield, 1 μL of isolated RNA was labeled with a RiboGreen™ RNA Quantitation kit (Molecular Probes, Eugene, Oregon) and concentrations were estimated with a fluorescence spectrophotometer F2500 (Hitachi Co., Tokyo, Japan) in 1 mL of total volume with water.

For microarray analysis, extracted total RNA samples were subjected to amplification, consisting of reverse tran-

scription and subsequent *in vitro* transcription, using a MessageAmp™ aRNA Kit (Ambion) with an oligo dT/T7 primer, according to the manufacturer's protocol. Total RNA samples from liver UFT sections were either subjected to one- or two-step amplification, and those from methacarn-fixed liver PET sections were subjected to two-step amplification. For expression analysis with the microdissected MPOA, two-step amplification was performed. For one-step amplification, 5 μg of total RNA was subjected to one-round of aRNA amplification. For the two-step amplification, 50 ng of total RNA was subjected to first-round amplification, and resultant aRNAs of 150–200 ng were subjected to second-round amplification. During the second *in vitro* transcription, generating aRNAs were labeled with biotin-UTP and biotin-CTP (Enzo Biochem, Farmingdale, NY).

For normalization of transcript levels with reference to amplification efficiency, an *in vitro* transcribed spike RNA from pGIBS-PHE (American Type Culture Collection, Manassas, VA), a short fragment of *Bacillus subtilis* (accession no. M24537 in GenBank/EMBL data bank), was added to the extracted total RNA at 3.76 pg/μg.

After the second-round amplification, 20 μg of biotinylated aRNA was denatured at 94°C for 35 min in fragmentation buffer (4×10^{-2} *M* Tris-acetate, pH 8.1, 1×10^{-7} *M* KOAc, 3×10^{-2} *M* MgOAc) and subjected to hybridization in a mixture containing control cRNAs (Affymetrix, Santa Clara, CA). Aliquots of 200 μL containing approximately 15 μg of aRNA were hybridized with GeneChip® Rat Genome U34A Arrays (Affymetrix) at 45°C for 18 h, stained with streptavidin/R-phycoerythrin conjugates (Molecular Probes), and then scanned with a GeneChip® Scanner 3000 (Affymetrix). Individual samples were subjected to analysis with individual microarrays in both the validation study and the MPOA-specific gene expression profiling study (n = 3/group for comparison in each study).

Real-Time RT-PCR

Quantitative real-time RT-PCR was performed for confirmation of expression values obtained with microarrays using ABI Prism 7700 (Applied Biosystems Japan, Tokyo, Japan). In a separate microarray study, to investigate gene expression changes in microdissected MPOA of rat neonates that have been administered 0.01–0.5 ppm ethinylestradiol through the maternal diet, we selected two genes, i.e., thymosin β4 and GTP-binding protein (Gαi2), showing profound sex differences in basal expression. Gene specific primers for thymosin β4 (accession no. NM_031136 in the GenBank/EMBL data banks) and Gαi2 (M12672) as well as corresponding TaqMan® MGB probes (6-FAM™-dye-labeled) were obtained from Assays-on-Demand™ Gene Expression Products (Applied Biosystems Japan). Reverse transcription was performed using 100 ng of first-round aRNAs prepared for microarray analysis containing spike RNA with a high-capacity cDNA Archive Kit (Applied Biosystems Japan) in a 100 μL total reaction volume. Real-time PCR was performed in a 50 μL reaction volume using the TaqMan probe detection system with 25 μL of TaqMan® Universal PCR Master Mix (Applied Biosystems Japan) and 2.5 μL each of target primer mix and RT product. Cycle parameters with this system were: single step of 50°C for 2 min, initial activation at 95°C for 10 min, 45 cycles of 15 sec at 95°C, and 60 sec at 60°C. For quantitation of expression data, a standard curve method was applied using first-round amplified aRNAs from a male MPOA as a standard sample.

For the spike gene (*Bacillus subtilis*), *in vitro* amplified transcript levels were measured by one-step real-time RT-PCR using the SYBR® Green detection system in a 50 μL total reaction mixture containing 25 μL of 2× QuantiTect™ SYBR® Green PCR Master Mix (QIAGEN), 8 ng of first-round amplified aRNA, multiscribe RTase (17.5 units), RNase inhibitor (20 units), and 2.5×10^{-7} *M* of primers. Cycle parameters in this system were as follows: 48°C for 30 min, 95°C for 10 min, 45 cycles of 15 sec at 95°C, and 60 sec at 60°C. The primer set for the spike gene, 5′-AGCGCCCCGGACTGA-3′ (forward; nucleotides 3152–3166), and 5′-CTCTAGGCCCAAAACGACCTT-3′ (reverse; nucleotides 3107–3127), was designed using Primer Express® software (Version 2.0; Applied Biosystems Japan).

Immunohistochemical Analysis

Whole brains of male and female neonates injected with EB or vehicle at PND 1 and obtained on PND 2 were subjected to fixation in Bouin's solution overnight (n = 4/sex/group). Coronal brain slices including the hypothalamus were trimmed and paraffin-embedded, and 3-μm serial sections were prepared for localization of the MPOA including the SDN-POA with HE-stained sections each one prepared in every 10 sections.

Immunohistochemistry was performed with antibodies against poly(ADP-ribose) polymerase (PARP) (rabbit IgG, 50× dilution; Santa Cruz Biotechnology, Santa Cruz, CA), glutamate receptor (GluR) 1 (rabbit immunoaffinity purified IgG, 1 μg/mL; Upstate, Charlottesville, VA), GluR5 (rabbit polyclonal IgG, 100× dilution; Upstate), GluR6/7 (rabbit immunoaffinity purified IgG, 5 μg/mL; Upstate), microtubule-associated protein (MAP) 2 (mouse monoclonal IgG_1, 400× dilution; Chemicon International, Inc, Temecula, CA), and metallothionein-1/2 (MT-1/2; clone E9, mouse $IgG_{1\kappa}$, 400× dilution; DakoCytomation, Carpinteria, CA). The PARP antibody can detect PARP-1, and to a lesser extent PARP-2, according to the manufacturer's product information. For detection of GluR1, GluR5, and GluR6/7, deparaffinized sections were subjected to microwave treatment, four times for 3 min in 1×10^{-2} *M* citrate buffer (pH 6.0), according to the recommendation in the manufacturer's protocol. For MAP2, microwave treatment was performed twice for 3 min in the same citrate buffer. Nonspecific endogenous peroxidase activity was blocked by treatment with 0.9% hydrogen peroxide in absolute methanol for 10 min. After masking with normal goat (for rabbit polyclonal antibodies) or horse (for mouse monoclonal antibod-

Table 1 Comparison of the Expression Status of Genes in Microarrays Between aRNA Samples Prepared from UFT and Methacarn-Fixed PET[a]

Tissue Status	UFT		Methacarn-Fixed PET
aRNA Sample	1× amplified	2× amplified	2× amplified
Rates with gene probes for each expression status (%)			
Present	40.3	36.9	36.4
Absent	57.5	60.9	61.5
Marginal	2.2	2.2	2.1
Signal ratio with the GAPDH gene (3′/5′, × fold)	1.1	12.3	11.3

aRNA, antisense RNA; UFT, unfixed frozen tissue; PET, paraffin-embedded tissue; GAPDH, glyceraldehyde-3-phosphate dehydrogenase.
[a] Liver tissue of a rat treated daily with sodium phenobarbital (80 mg/kg body weight, s.c.) for three days was used.

ies) serum, sections were incubated with primary antibodies, overnight at 4°C, and subsequently with biotinylated secondary antibody for 60 min at room temperature. All antibodies used were diluted with 0.5% casein in PBS before application. Immunodetection was carried out with the horseradish peroxidase–avidin–biotin complex utilizing a VECTASTAIN® Elite ABC kit (Vector Laboratories, Burlingame, CA), with 3,3′-diaminobenzidine/H_2O_2 as the chromogen. Sections were counterstained with hematoxylin for microscopic examination. For quantitative measurement of the numbers of nuclei immunoreactive for PARP, bilateral portions of a 250 × 250 μm area covering the SDN region were subjected to analysis under 200× magnification. Also, nuclei immunoreactive for MT-1/2 were counted in bilateral MPOAs by randomly selecting three fields (125 × 125 μm area) on each side under 400× magnification. For each antigen (PARP and MT-1/2), mean ratios of nuclear immunoreactive cells to the total cells counted in each side were estimated.

Data Analysis

Scanned output files of microarrays were visually inspected for hybridization artifacts, and then expression signals for each gene were measured by calculating pixel intensities using a Microarray Suite software package (Version 5.0, Affymetrix). With this software, the expression status of each gene, whether present, absent, or marginally expressed, was judged. Exclusion of genes showing absence in at least three of six samples of the two groups for comparison of expression, normalization of expression data, and statistical comparisons were performed using GeneSpring™ software (Version 5; Silicon Genetics; Redwood City, CA). For microarray data in the validation study of expression fidelity with methacarn-fixed PET specimens, per chip normalization was performed by dividing the signal strength for each gene with the level of the 50th percentile of the measurement in the chip, and per gene normalization with average signal strength of the identical gene of three 1×-amplified aRNAs samples from UFTs. With regard to the microarray data for microdissected MPOA, per chip normalization was performed by dividing the signal strength of each gene by the level of the spike RNA signal in each sample, and per gene normalization with average signal strength of the identical gene in three untreated control samples. Average relative expression values were determined for each gene in the treatment group, and genes showing expression changes with ≥2-fold differences were first estimated. Then, comparison of expression data between the untreated controls and each treatment group was performed using Student's *t*-test with multiple testing corrections applying Benjamini and Hochberg false positive discovery rate calculations, and genes showing statistical significance with a p value <0.05 were selected.

To assess fidelity of expression patterns in microarrays between the 2×-amplified aRNA samples from methacarn-fixed liver PETs and 1×- and 2×-amplified samples from liver UFTs, Pearson's correlation coefficients (r) for each combination were estimated using all genes included in the array.

For the real-time RT-PCR data, expression values were normalized to the amplification efficiency of the first-round *in vitro* transcription by dividing the expression values with the signal level of spike RNA included in each sample. Differences in expression levels between sexes were analyzed by the Student's *t*-test, when the variance proved to be homogeneous among groups using the test for equal variance. If a significant difference in the variance was observed, a Welch's *t*-test was performed.

Morphometrically analyzed data for nuclear immunoreactive cell ratios of PARP and MT-1/2 were compared by Student's and Welch's *t*-tests. Regarding immunoreactivities on which morphometric analysis could not be applied, total incidence of immunoreactive cases and grades of intensity were visually analyzed and statistically compared using the Fisher's exact probability test and Mann–Whitney's *U*-test, respectively.

RESULTS

Expression Fidelity in Methacarn-fixed PETs

Expression fidelity of the microdissected small tissue samples in microarray analysis might be influenced by tissue processing for microdissection and/or multiround amplification. To clarify the effect of tissue processing for microdissection (methacarn-fixation and following paraffin-embedding) on the expression

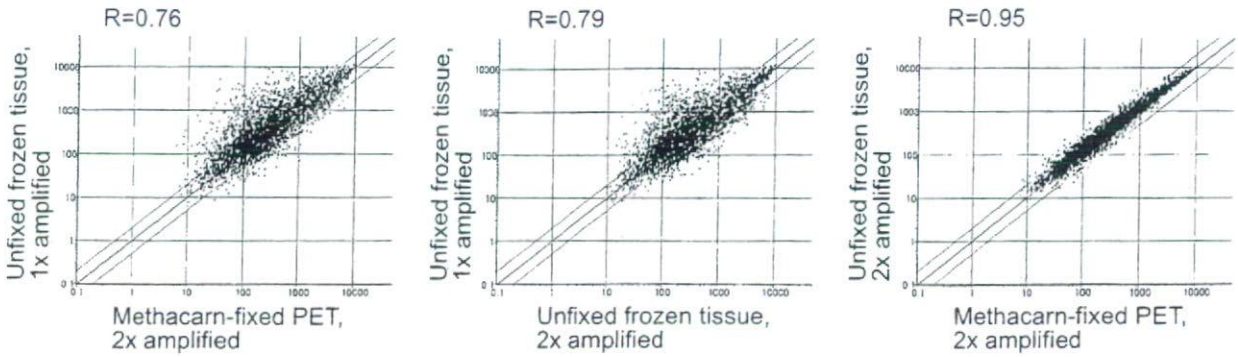

Figure 2 Scatter plot analysis of gene expression profiles of aRNA samples derived from methacarn-fixed PET and UFT of rat liver.

fidelity after 2×-amplification, expression in the second-round amplified aRNA samples was compared with that obtained from the 1×- or 2×-amplified aRNAs from UFT. With the 8799 probes included in the array used, percentages of expression status (present, absent, and marginal) were similar among aRNA-preparations irrespective of the tissue status and the amplification cycle (Table 1). However, preferential amplification of the 3′ portions was evident with 2× amplification in both UFT and methacarn-fixed PET cases (Table 1). By scatter plot analysis, high correlations were observed in the expression profiles between the 2×-amplified aRNAs from methacarn-fixed PET and UFT ($r = 0.95$, $n = 3$; Fig. 2). When the correlation of gene expression levels was examined between the 1×-amplified aRNAs from UFT and 2×-amplified ones from either methacarn-fixed PET or UFT, r values were similar, but relatively low when compared with the value for the correlation between the two 2× amplified examples, indicating a lowered expression fidelity in the methacarn-fixed PET because of the second-round amplification. When the number of genes showing presence was examined for 2×-amplified methacarn-fixed PET and 1×-amplified UFT aRNAs, 3173 probes were positive in common (as shown in Fig. 3). The numbers of probes showing presence solely in the methacarn-fixed PET (2× amplified) and UFT (1× amplified) were 373 and 822, respectively, suggesting that 10.5% of the total genes exhibiting presence in the 2×-amplified samples should be regarded to be false positive, and that 20.6% of the present genes in the 1×-amplified samples from UFT lost their signals after two-round amplification. It is possible that the distance from the poly(A) tail to the positions of the probes may affect the expression status of each gene after the second-round *in vitro* transcription due to preferential amplification of the 3′-terminal portion. Among genes showing presence solely in the methacarn-fixed PET (2× amplified) and UFT (1× amplified), sequence information including the full 3′-untranslated region from the poly(A) tail was available for six and five genes, respectively. The mean distances from the 5′-end of the probes (both 5′- and 3′-most probes) to the 5′-end of poly(A) tail expressed as the number of nucleotides were examined for these (Table 2), and as expected, they were shorter with 2×-amplified aRNA samples from methacarn-fixed PET than with their 1×-amplified counterparts from UFT. These results indicate that the decline in expression fidelity with 2×-amplified samples is mainly due to preferential amplification at the 3′-portions by the second-round amplification and methacarn fixation and paraffin-embedding did not apparently affect the fidelity.

Gene Expression Profiles of MPOA of Neonates Acutely Treated with EB or FA

In the MPOAs at PND 2, about 3600 genes showed presence in both sexes in untreated controls. Sex dif-

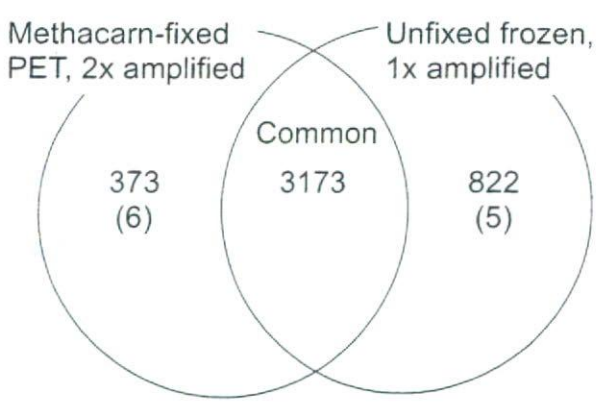

Figure 3 Gene populations showing presence with aRNA samples 2×-amplified from methacarn-fixed PET and 1×-amplified from UFT.

Table 2 Mean Distance from the Probes to the Poly(A) Tail Positions of Genes Showing Presence Solely in the UFT or Methacarn-Fixed PET[a]

aRNA Sample	UFT, 1× amplified	Methacarn-Fixed PET, 2× amplified
Mean distance from the 5′ end of the poly(A) tail (bp)		
No. of genes examined[b]	6	5
3′ end of the 5′ most probe	847	318[c]
3′ end of the 3′ most probe	569	97[c]

aRNA, antisense RNA; UFT, unfixed frozen tissue; PET, paraffin-embedded tissue.

[a] Genes obtained from microarray data in Table 1 were examined.

[b] All genes with sequence information for the 3′-untranslated region were examined.

[c] Significantly different from the unfixed frozen samples ($p < 0.01$).

ferences for male- or female-biased expression were found for 21% and 6% of all present genes, respectively (≥2-fold; Table 3). On EB-treatment, females demonstrated a greater number of genes with expression change. In males, up-regulation by EB was found for only 25 genes, all of them within 2- to 5-fold, and no genes showed down-regulation. In females, up-regulation was detected for a total of 586 genes after EB-treatment (≥2-fold), with 52 genes exhibiting ≥5-fold increase. When compared with up-regulated genes, down-regulated examples were fewer in number in females, with a total of 187 genes showing ≤1/2-fold down-regulation when compared with the vehicle control level. Among them, 33 genes showed ≤1/5-fold down-regulation when compared with vehicle controls. Relatively small numbers of genes showed altered expression on FA-treatment in both sexes. In males, only two and three genes showed up- and down-regulation, respectively (2- to 5-fold change), and in females, three and 22, all of them exhibiting 2- to 5-fold change, except for one gene with ≤1/5-fold up- and down-regulation, respectively.

Among genes showing male-biased expression (≥2-fold difference; 740 genes in total), 59% of them exhibited up-regulation on EB-treatment in females (≥2-fold; 437 genes in total), one of them also exhibiting up-regulation by FA in males (as shown in Fig. 4). One example alone showed down-regulation by FA in males. On the other hand, among genes showing female-biased expression (≥2-fold difference; 203 genes in total), 55% of them exhibited down-regulation by EB in females (≤1/2-fold; 111 genes in total). Among them, a total of 10 genes also showed altered expression by FA; nine genes down-regulated in females and one gene up-regulated in males. On the other hand, five female-predominant genes exhibited up-regulation by EB in males, four of them also showing down-regulation by EB in females, with one gene each further showing down-regulation in females and up-regulation in males by FA-treatment.

When genes that demonstrated changed expression levels in both sexes by the chemical treatments were examined, four genes encoding the LINE retrotransposable element 3, L1Rn B6 repetitive DNA element, ADP-ribosyltransferase (adprt) 1, and NonO/p54nrb homolog, exhibited up-regulation in males and down-regulation in females by EB-treatment and also female-biased expression (Table 4). Expression levels for genes showing male-biased expression were not affected by EB. FA-treatment did not alter the expression level of any gene involving both sexes.

Table 5 shows the list of genes showing altered expression in the MPOA of either sex common to both chemicals. Among the total of 15, 12 showed down-regulation in females common to EB and FA, eight of them exhibiting female-biased expression, i.e., for protein tyrosine phosphatase, receptor type, F (*PTPRF*); DAP-like kinase (*dlk*); glutamate receptor, kainate receptor subunit (KA1); dyskeratosis congenita 1 (*dyskerin*); L1Rn B6 repetitive DNA element; *MAP2*; expressed sequence tag (EST), similar to the mouse estrogen-responsive finger protein (*efp*); and glutamate receptor, ionotropic, AMPA subtype (GluR1).

Table 3 Number of Genes Showing Sex Differences in Basal Expression as well as Alteration After EB or FA Treatment in the Neonatal MPOA ($p < 0.05$)

Difference/Change (× fold)	2–5	≥5
Sex difference		
Males > females	676	64
Females > males	176	27
Altered by EB		
Males		
Up-regulated	25	0
Down-regulated	0	0
Females		
Up-regulated	534	52
Down-regulated	154	33
Altered by FA		
Males		
Up-regulated	2	0
Down-regulated	3	0
Females		
Up-regulated	3	0
Down-regulated	22	0

EB, estradiol benzoate; FA, flutamide; MPOA, medial preoptic area.

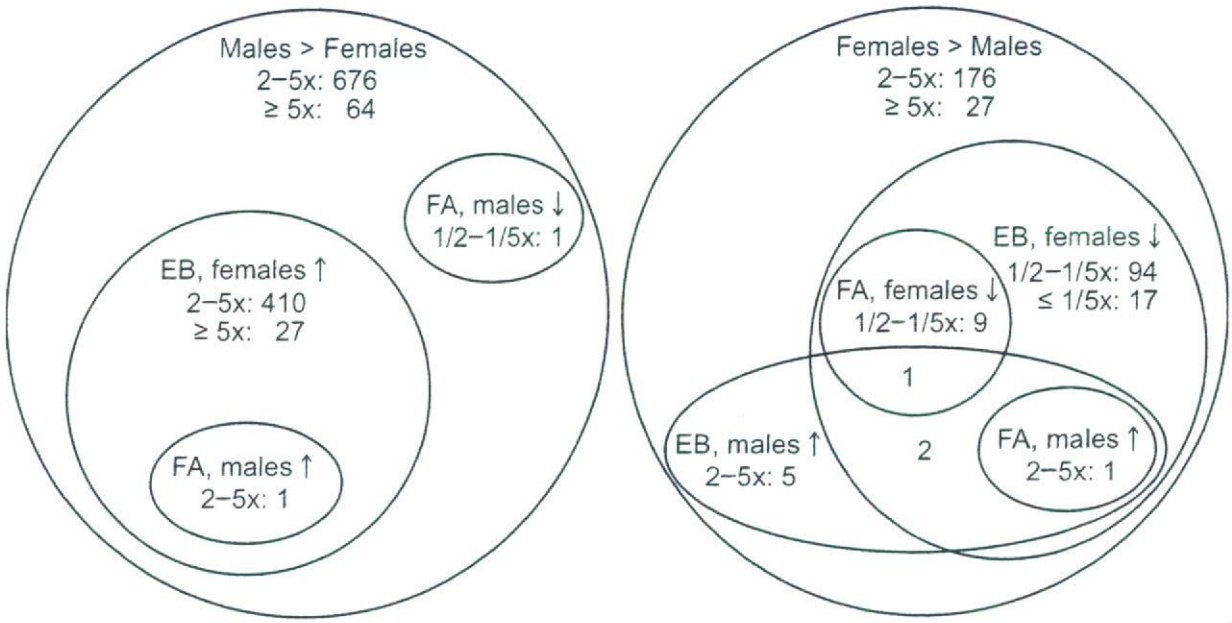

Figure 4 Distribution of gene populations showing altered expression with EB and/or FA-treatment among those showing sex differences in expression in the neonatal MPOA.

Interestingly, two subtypes of glutamate receptors, KA1 and GluR1, exhibited this particular expression pattern, the former being detected with two different probe sets (accession nos. U08257 and X59996). Without showing sex differences in the basal expression, expression of five genes were influenced by EB and FA, the following four exhibiting down-regulation in females with both chemicals: myeloid/lymphoid or mixed-lineage leukemia (trithorax (drosophila) homolog); translocated to, 3; cyclin D1; serine/threonine kinase 25; and neurotrimin. On the other hand, one EST (accession no. AI639097) showed up-regulation by EB and down-regulation by FA in females. Among the genes listed in Table 5, up-regulated examples were rather few and the magnitude of up-regulation was within 2- to 3-fold. In addition to the altered expression involving both sexes after EB treatment (see above), two genes showed altered expression with FA, i.e., down-regulation of the L1Rn B6 repetitive DNA element in females, and up-regulation of the LINE retrotransposable element 3 in males. Among those showing male-biased expression, there was only one with altered expression due to both EB and FA. MT1a transcripts showed up-regulation by EB in females and also by FA in males.

Fig. 5 shows mRNA expression data for two genes by real-time RT-PCR regarding sex differences in the neonatal MPOAs observed with microarrays. Both thymosin $\beta 4$ and $G\alpha i2$ mRNAs exhibited strong male-biased expression at PND 2, with 8.9- and 7.1-fold higher levels than in females. Real-time RT-PCR results confirmed this sex difference.

Immunoreactivity of Protein Signals

Fig. 6 shows representative figures for immunohistochemical demonstration of protein signals in the MPOA with the anatomical location indicated in

Table 4 List of Genes Showing Altered Expression in the MPOA of Both Sexes by EB-Treatment (≥2-fold, $p < 0.05$)

Accession No.	Gene	Sex Difference (× fold)	Altered by EB (× fold *vs.* control) M	F
M13100	LINE retrotransposable element 3	M<F (2.9)	2.1	0.5
X07686	L1Rn B6 repetitive DNA element	M<F (3.8)	2.0	0.4
AA964849	ADP-ribosyltransferase (adprt) 1	M<F (3.3)	2.2	0.3
AF036335	NonO/p54nrb homolog	M<F (5.5)	3.2	<0.1

MPOA, medial preoptic area; EB, estradiol benzoate; FA, flutamide; M, males; F, females; EST, expressed sequence tag.

Table 5 List of Genes Showing Altered Expression in the MPOA Common to EB and FA (≥2-fold, $p < 0.05$)

Accession No.	Gene	Sex Difference (× fold)	Altered by EB (× fold *vs.* control)		Altered by FA (× fold *vs.* control)	
			M	F	M	F
M13100	LINE retrotransposable element 3	M<F (2.9)	2.1	0.5	2.2	–
U87960	Protein tyrosine phosphatase, receptor type, F (PTPRF); leukocyte common antigen receptor (LAR)	M<F (11.8)	–	0.1	–	0.4
AJ006971	DAP-like kinase (dlk)	M<F (6.4)	–	0.3	–	0.3
U08257 (X59996)	Glutamate receptor, ionotropic, kainite 4 (Grik4); Kainate receptor subunit (KA1)	M<F (5.8) (M<F (5.4))	– (–)	0.3 (0.2)	– (–)	0.5 (0.5)
AA892562	Dyskeratosis congenita 1, dyskerin (dkc1)	M<F (4.0)	–	0.4	–	0.4
X07686	L1Rn B6 repetitive DNA element	M<F (3.8)	2.0	0.4	–	0.2
X53455	Microtubule-associated protein 2 (MAP2)	M<F (3.5)	–	0.1	–	0.3
AA859593	EST, similar to mouse estrogen-responsive finger protein (efp)	M<F (3.4)	–	0.3	–	0.5
X17184	Glutamate receptor, ionotropic, AMPA subtype, GluR1	M<F (3.1)	–	0.3	–	0.5
AJ006295	Myeloid/lymphoid or mixed-lineage leukemia (trithorax (Drosophila) homolog); translocated to, 3 (mllt3); AF-9	–	–	0.4	–	0.5
AI231257	Cyclin D1	–	–	0.4	–	0.5
AA799791	Serine/threonine kinase 25 (STE20 homolog, yeast) (stk25)	–	–	0.4	–	0.4
U16845	Neurotrimin	–	–	0.5	–	0.5
AI639097	EST	–	–	2.2	–	0.5
AI176456	Metallothionein (MT1a)	M>F (2.8)	–	2.9	2.3	–

MPOA, medial preoptic area; EB, estradiol benzoate; FA, flutamide; M, males; F, females; EST, expressed sequence tag.

Figure 1. In the hypothalamus at PND 2, nuclear immunoreactivity of PARP, the protein product of the *adprt* gene (Skaper, 2003), was observed in the ventricular ependymal and subependymal cells around the third ventricle. On quantitative measurement of nuclear immunoreactivity at the SDN region, cases with higher grades of distribution were more frequent in female controls when compared with the males [Figs. 6(A,B) and 7]. EB-treatment increased and decreased the positive cell distribution in males and females, respectively [Figs. 6(C) and 7]. GluR1 immunoreactivity was observed in the cytoplasm and dendritic processes of neuronal cells, its staining intensity being mostly weak in the MPOAs, even in the positive cases, when compared with the other brain areas, such as the hippocampus, cerebral cortex, and striatum [Fig. 6(D)]. In the MPOAs of male controls, two out of four cases showed only minimal intensity of GluR1-immunoreactivity, and the other two showed negative results [Fig. 6(D), Table 6]. Although the intensity was minimal to slight, all control females showed positive immunoreactivity in their MPOAs [Fig. 6(E)]. EB-treatment did not alter the intensity in either sex [female: Fig. 6(F)]. With regard to GluR5, very faint immunoreactivity was observed in the dendritic processes in the striatum and bed nucleus, but staining was lacking in the MPOAs of both sexes, even with the EB treatment

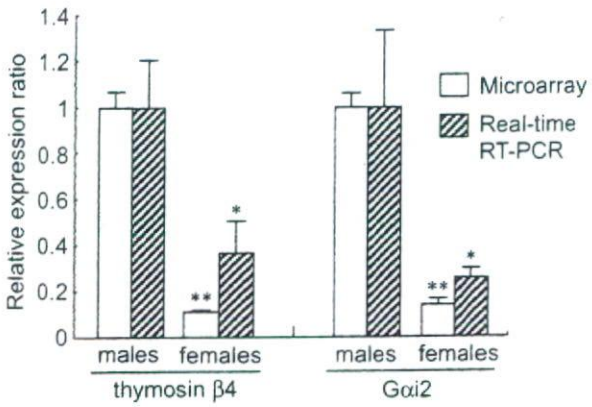

Figure 5 Confirmation of microarray data by real-time RT-PCR in the neonatal MPOA. Sex differences in the mRNA expression of thymosin $\beta 4$ and Gαi2 were analyzed. Significantly different from the male value in each detection system ($*p < 0.05$, $**p < 0.01$).

(Table 6). GluR6/7-immunoreactivity was observed in the cytoplasm of both neuronal and glial cells of the whole brain area, but there was no obvious change in terms of the distribution and intensity in the MPOAs, irrespective of the sex or EB treatment (Table 6). MAP2 immunoreactivity was observed in the whole dendritic processes with a fibrillary expression pattern, but there was no obvious change in terms of the distribution and intensity in the MPOAs, irrespective of the sex or EB treatment (Table 6). Strong cytoplasmic immunoreactivity of MT-1/2 was observed in the astrocytes located in the deep cortex and white matter of the cerebrum, hippocampal white matter, and striatum [Fig. 6(G)]. In other brain areas, MT-1/2-immunoreactivity was rather weak and sparse, and both nuclear and cytoplasmic. In the MPOAs, nuclear immunoreactivity predominated over cytoplasmic staining. On quantitative measurement of the nuclear immunoreactivity, the positive cell ratio was higher in males than in females, with increase in the latter on EB treatment [Figs. 6(G–I) and 7].

DISCUSSION

In the present validation study to establish a region-specific microarray analysis method using PET samples in combination with methacarn fixation, we found that gene expression profiles were very similar between 2×-amplified aRNAs from UFT and methacarn-fixed PET, and the deviation in expression data with the second-round amplification from the 1×-amplified aRNAs of UFT was mostly due to the preferential amplification of the 3′-terminal portion, irrespective of the tissue status. These results strongly indicate that methacarn fixation and subsequent paraffin embedding do not affect the expression fidelity in microarray analyses. Although it is still necessary to improve expression fidelity with second-round amplification, the results suggest an advantage of methacarn in combination with paraffin embedding for global gene expression analysis of microdissected cellular regions. It should be stressed that paraffin embedding is essential for preparation of serial sections necessary for microdissection of anatomically defined tissue areas.

Although the sex difference in the incidence of apoptosis in the SDN region that is believed to be re-

Figure 6 Immunoexpression patterns for PARP (panels A-C), GluR1 (panels D-F), and MT-1/2 (panels G-I), in the neonatal rat MPOA at PND 2. A. Note scattered PARP-immunoreactive nuclei (arrowheads) in paraventricular cells of a control male. The inset shows a high-power view of the nuclear weak immunoreactivity in the same area. B. Distribution of PARP-weakly immunoreactive cell nuclei in a control female. Note accumulation of positive cells in the SDN region (arrow). C. Lack of PARP-immunoreactive cells in most paraventricular and SDN regions in an EB-treated female. D. Very weak, mostly negative GluR1-immunoreactivity in the cytoplasmic processes of neurons in a control male. The inset shows strong immunoreactivity in the cytoplasm and dendritic processes of neuronal cells of the cerebral cortex of the same brain section. E. Slight intensity of GluR1-immunoreactivity in cytoplasmic processes of neurons in a control female. The inset shows a high-power view of the immunoreactivity in cytoplasmic processes of the same area. F. Minimal degree of GluR1-immunoreactivity in an EB-treated female. G. Diffuse immunoexpression of MT-1/2 in a control male. The expression pattern is mostly nuclear, and both astrocytic (arrowheads) and neuronal (arrows) populations as well as ependymal cells (*) show apparent immunoreactivity. The inset shows strong expression in cytoplasmic processes of astrocytes in the deep cerebral cortex of the same brain section. H. Scattered weak nuclear immunoreactivity of MT-1/2 in a control female. I. Diffuse nuclear and scattered cytoplasmic distribution of immunoreactive cells in an EB-treated female. The inset shows a high power view of both nuclear and cytoplasmic immunoreactivity in the same area. Bar = 50 μm, including insets.

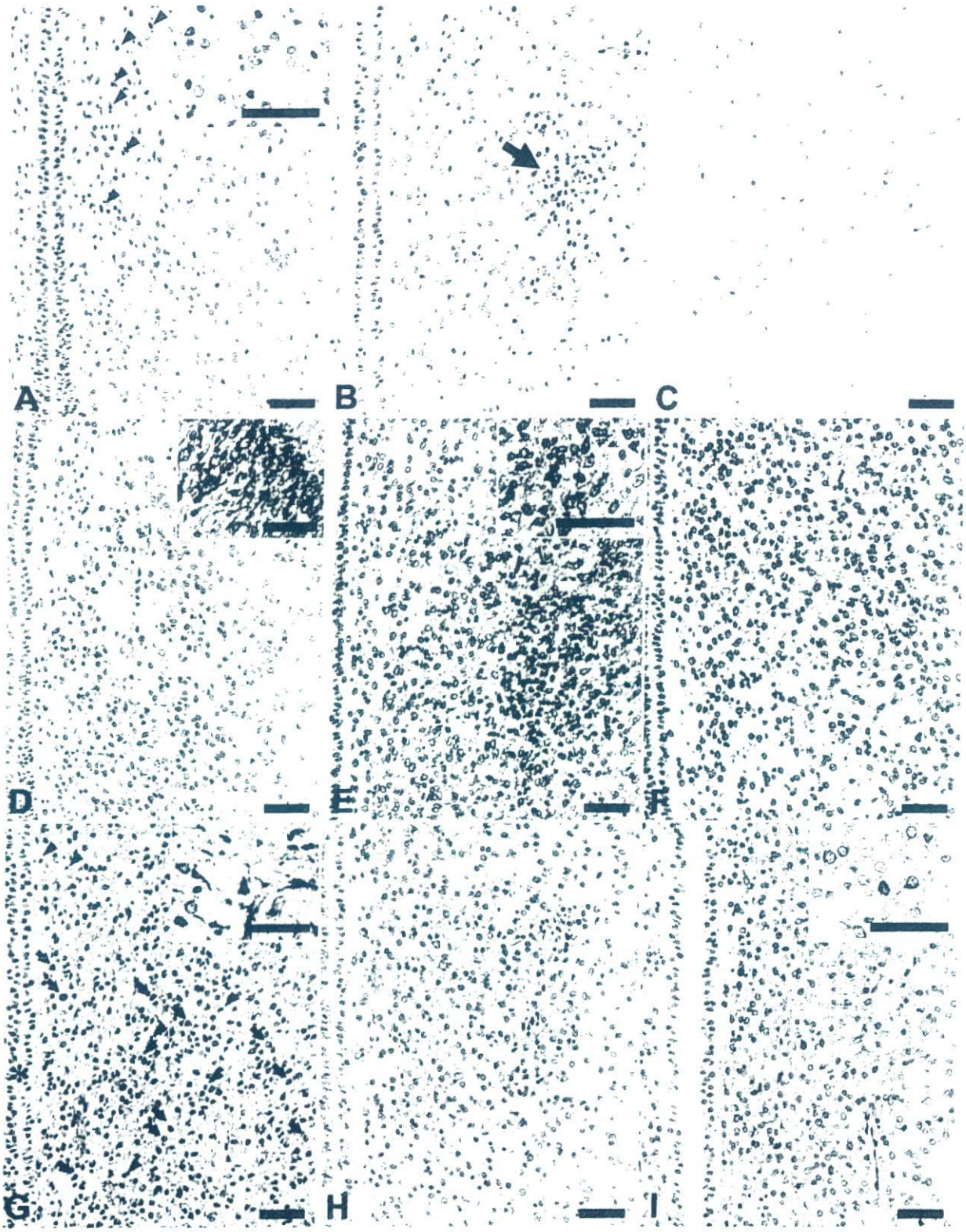

Figure 6

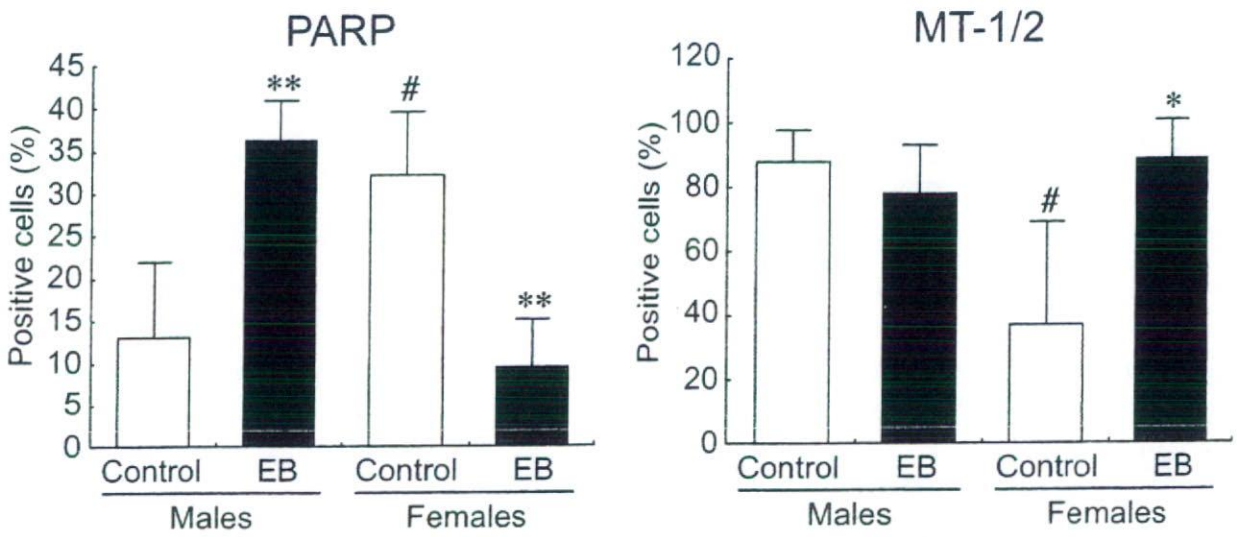

Figure 7 Nuclear immunoreactive cell percentages for PARP and MT-1/2 in neonatal rat MPOAs at PND 2. Significantly different from the corresponding controls ($*p < 0.05$, $**p < 0.01$). Significantly different from the male controls ($^{\#}p < 0.05$).

sponsible for subsequent sexually dimorphic development of this nucleus first occurs between PNDs seven and 10 (Davis et al., 1996), the number of genes exhibiting male-biased constitutive expression was much higher than in females at time points as early as PND 2 in the present study. This sex difference is presumably the reflection of growth and/or antiapoptotic effects for male-type large SDN under the influence of estradiol generated by aromatase from testosterone perinatally secreted from the developing testis (Matsumoto et al., 2000). Regarding responses to chemicals, the number of genes showing altered expression by EB or FA was far greater in females than in males, suggesting an effect on normal female sexual differentiation. Moreover, approximately 60% of genes showing male or female-biased expression demonstrated altered levels with EB in females, pointing to an involvement of genes necessary for normal processes of male- or female-type brain sexual differentiation in its disruptive effects. It is well known that the perinatal/neonatal treatment of animals with estrogenic compounds can affect sexual development of both sexes, resulting in reproductive dysfunction (Nagao et al., 1999; Odum et al., 2002; Tsukahara et al., 2003; Shibutani et al., 2005). With regard to the effects of antiandrogens, disruption of sexual development has generally been apparent in males, but the situation is largely unclear for females (Gray and Kelce, 1996; Wolf et al., 2004). With FA, however, prenatal exposure affects the volume of the anteroventral periventricular nucleus (AVPVN) in female rats (Lund et al., 2000) and the female sexual behavior in guinea pigs (Thornton et al., 1991). In addition, FA exerts antiprogestin activity (Chandrasekhar and Armstrong, 1989; Dukes et al., 2000).

Table 6 Immunoreactivity of Protein Signals in the MPOA of Neonatal Rats Treated with EB[a]

	Males		Females	
Antigen	Control	EB	Control	EB
Number of animals	4	4	4	4
GluR1 (±/+)[b]	2[c](2/0)[d]	3(3/0)	4(3/1)	3(3/0)
GluR5 (present)	0	0	0	0
GluR6/7 (±/+/++)[b]	4(2/2/0)	4(0/4/0)	4(0/3/1)	4(2/2/0)
MAP2 (±/+/++)[b]	4(0/3/1)	4(0/3/1)	4(2/2/0)	4(2/2/0)

Protein signals with immunoexpression patterns for which morphometric analysis could not be applied were analyzed by visual estimation of the grade of intensity of immunoreactivity in the MPOA. MPOA, medial preoptic area; EB, estradiol benzoate; GluR1, glutamate receptor 1; GluR5, glutamate receptor 5; GluR6/7; glutamate receptor 6/7; MAP2, microtubule-associated protein 2.

[a] Rat neonates treated with EB at 10 μg/pup or vehicle on PND1 and sacrificed 24 h later were examined.

[b] Grades of intensity of immunoreactivity: ±, minimal; +, slight; ++, moderate; and +++, prominent.

[c] Total number of animals showing positive immunoreactivity.

[d] Number of animals with each grade.

Our search for genes showing altered expression by EB or FA revealed a total of four female-predominant genes with change by EB in both sexes, all up-regulated in males and down-regulated in females. Two of them are long interspersed repetitive DNAs, L1, or LINE, a class of mobile genetic elements named retrotransposons which can be amplified by retroposition, i.e. by a mechanism similar to that observed with retroviruses (Servomaa and Rytoamaa,

1990). This group of retrotransposons includes regulatory signals and encodes two proteins, a RNA-binding protein and an integrase-replicase (Han and Boeke, 2005). The human genome contains about 500,000 LINES, accounting for roughly 17% of the total (Haoudi et al., 2004). Various environmental factors, such as steroid hormone-like agents and stressors can facilitate L1 transcription to alter cellular functions (Servomaa and Rytoamaa, 1990; Morales et al., 2002, 2003). Moreover, a regulatory role of L1 repeats at the promoter region has been reported with estrogen-related gene transcription (Hardy et al., 2001). During neuronal differentiation, retrotransposition events can alter the expression of neuronal genes, which, in turn, can influence neuronal cell fate (Muotri et al., 2005). Thus, the sex differences in the retrotransposon expression in the developing MPOA apparent here suggest roles in sex-dependent gene expression control, and alteration in their expression status due to EB may indicate roles as upstream regulators of genes necessary for brain sexual differentiation.

Two other genes showing up-regulation in males and down-regulation in females with EB, as well as female-biased expression, were *adprt1* and *NonO/p54nrb*. *Adprt1* encodes PARP-1, an abundant nuclear enzyme that is activated primarily by DNA damage; however, its excessive activation can lead to cell death (Skaper, 2003; Koh et al., 2005). Interestingly, sex differences exist regarding PARP-1 activation as well as nitric oxide toxicity in a mouse ischemic neurotoxicity model (McCullough et al., 2005). In the periventricular cell populations, poly(ADP-ribosyl)ation is basally activated by DNA strand breaks reflecting glutamate-nitric oxide neurotransmission (Pieper et al., 2000). In the present study, the measured level of PARP-immunoexpression at the SDN region was in line with the microarray data, suggesting an induction of subsequent programmed cell death in the female SDN-POA (Davis et al., 1996). Similarly, increased expression of PARP in males and its decrease in females with EB here may be linked to the decreased SDN volume in males in later life (Shibutani et al., 2005) and the decreased apoptosis in the female SDN after EB injection (Arai et al., 1996), respectively. NonO/p54nrb has been implicated in a variety of nuclear processes (Proteau et al., 2005). Indeed, this protein is known to act as a transcription factor necessary for adrenocortical steroidogenesis (Sewer et al., 2002), and as a transcriptional co-activator of the human androgen receptor (AR; Ishitani et al., 2003).

In the present study, a total of 15 genes exhibited altered expression due to FA in either sex, in addition to alteration by EB. Among them, 10 genes also exhibited sex differences in expression including the two genes for retrotransposons mentioned earlier. Interestingly, many of the 15 genes exhibited similar expression patterns with EB and FA, most being down-regulated in females, suggesting a common mechanism of action of the two chemicals. The following seven genes showed this particular expression pattern, in addition to the L1 repeat mentioned earlier: *PTPRF*/leukocyte common antigen-related (LAR) protein, *dlk*, two kinds of glutamate receptors, *dyskerin*, *MAP2*, and *efp*. In males, neonatal estrogen treatment affects the developing testis to suppress androgen secretion, presumably resulting in effects similar to antiandrogenicity on postnatal development (Atanassova et al., 1999). On the other hand, FA in the 20-day pubertal female assay using rats has been shown to exert ER-agonist activity on female sexual development, attributed to an imbalance between endogenous estrogenic and androgenic stimuli in the target organs (Kim et al., 2002).

Regarding glutamate receptors, mRNA expression of GluR1, the AMPA subtype found here with altered expression, is up-regulated in the AVPVN by estrogen in ovariectomized juvenile female rats (Gu et al., 1999). Hypothalamic GluR1 protein level was also increased in gonadectomized and estrogen-treated adult rats irrespective of the sex (Diano et al., 1997). Different from our female neonates, these results suggest that estrogen could up-regulate GluR1 levels in the juvenile/adult rat hypothalamus, probably through a different mechanism from that during sexual differentiation. In the female MPOA, we here could detect a slight, but nonsignificant increase in GluR1-immunoreactive cases when compared with those in males. Although we could not examine immunohistochemical localization of KA1 subunit here, other kainate receptor subtypes (GluR5, 6, and 7) have shown, in a study using adult rats, to be expressed in tanycytes, astrocytes, and neurons of the arcuate nucleus, with co-expression of AR or ER found in neurons in males and females, respectively (Diano et al., 1998). However, we could not detect any sex difference or EB-induced effect on the immunoreactivity of GluR5 or GluR6/7 in the neonatal MPOA.

PTPRF/LAR is a widely expressed tyrosine phosphatase that has been implicated in the regulation of a diverse range of signaling pathways, such as in the development and maintenance of excitatory synapses, and interestingly, disruption of its function results in reduction of surface AMPA receptors (Mooney and LeVea, 2003; Dunah et al., 2005). In the present study, AMPA subtype GluR1, as mentioned earlier, showed similar responses to EB and FA as well as a sex differ-

ence in mRNA expression, suggesting a coordinated action of PTPRF/LAR and AMPA receptors during brain sexual differentiation and its disruption.

MAP2 contributes to regulation of cytoskeletal organization and dynamics, and is expressed mainly in dendritic processes of neurons (Maccioni and Cambiazo, 1995). Posttranscriptional control of MAP2 expression has been reported in the female rat hippocampus in response to estrogen treatment or during the estrous cycle (Reyna-Neyra et al., 2002, 2004). Interestingly, estrogen can induce dendrite spines in the developing rat POA through activation of AMPA-kainate receptors by glutamate that may originate from astrocytes (Amateau and McCarthy, 2002). Inconsistent with the microarray data, MAP2-immunoreactivity in the neonatal MPOA here lacked any sex difference or change in expression on chemical treatment as in the case with above-mentioned GluR5 and GluR6/7.

Efp, a target gene product of ERα, is a RING-finger-dependent ubiquitin ligase that targets proteolysis of 14-3-3σ, a negative cell cycle regulator that causes G2 arrest (Urano et al., 2002), and is considered essential for estrogen-dependent tumor cell proliferation (Horie et al., 2003). This gene product is distributed mainly in estrogen-sensitive organs/tissues associated with ER co-expression (Orimo et al., 1995; Shimada et al., 2004). Dlk is a nuclear serine/threonine-specific kinase that has been implicated in the regulation of apoptosis by relocation to the cytoplasm, but its nuclear location has been suggestive of the roles for mitosis and cytokinesis (Preuss et al., 2003). Dyskerin, a nucleolar protein that modifies specific uridine residues of rRNA, also acting as a component of the telomerase complex, is a target molecule for skin and bone marrow failure syndrome called dyskeratosis congenita in human (Marrone et al., 2005). Dyskerin transcripts distribute ubiquitously in embryo-fetal tissues with notably high levels in epithelial and neural tissues (Heiss et al., 2000).

As a unique gene showing male-biased expression and increase with EB in females and decrease with FA in males, *MT1a* is of interest. MTs are considered to be important metal-binding proteins active in defense against heavy metal toxicity (Sogawa et al., 2001), and four major MT isoforms have so far been identified. In the present study, judging from the sequence information (accession no. AI176456) for the MT probes, either MT1 or 2 was suggested to be responsible for the particular expression pattern. Sex steroid-related expression changes in MT1 and/or 2 have been reported in the liver or brain of mice (Sogawa et al., 2001; Beltramini et al., 2004). In the brain, MT1 and 2 are expressed mainly in nonneuronal cells (Suzuki et al., 1994; Hidalgo et al., 2001), but certain levels are also found in neurons (Xie et al., 2004); as well as cytoplasmic expression, nuclear localization of MT has been reported in developing brain (Suzuki et al., 1994). Interestingly, kainic acid treatment can selectively induce MT1 in neurons and MT2 in glial cells in rats (Kim et al., 2003). Although the immunoreactivity of MT-1/2 was rather weak when compared with other brain areas and a nuclear expression was predominant in the neonatal MPOA here, male predominance may reflect a neuroprotective function, and expression changes due to EB and FA could indicate alteration in the regional hormonal environment in response to treatment.

In summary, we here established the basis for a global gene expression profiling method using paraffin-embedded, histologically defined small tissue areas with methacarn as a fixative. A male predominance in the number of genes showing constitutively higher expression suggestive of sex steroidal effects on the neonatal male MPOA was detected. Upon treatment with EB, many genes showing sex differences in expression demonstrated altered levels in females, in line with involvement of genes necessary for brain sexual differentiation in its disruption. Moreover, many genes commonly affected by EB and FA showed down-regulation in females with these drugs, suggesting common mechanisms shared between estrogenic and anti-androgenic chemicals in induction of endocrine center disruption in females, at least in early stages.

We thank Mrs. Keiko Kuroiwa for her technical assistance in conducting the immunohistochemical study. Dr. Lee was an Awardee of a Postdoctoral Fellowship from the Japan Society for the Promotion of Science during the performance of the study.

REFERENCES

Amateau SK, McCarthy MM. 2002. A novel mechanism of dendritic spine plasticity involving estradiol induction of prostaglandin-E_2. J Neurosci 22:8586–8596.

Arai Y, Sekine Y, Murakami S. 1996. Estrogen and apoptosis in the developing sexually dimorphic preoptic area in female rats. Neurosci Res 25:403–407.

Atanassova N, McKinnell C, Walker M, Turner KJ, Fisher JS, Morley M, Millar MR, et al. 1999. Permanent effects of neonatal estrogen exposure in rats on reproductive hormone levels, Sertoli cell number, and the efficiency of spermatogenesis in adulthood. Endocrinology 140:5364–5373.

Beltramini M, Zambenedetti P, Wittkowski W, Zatta P. 2004. Effects of steroid hormones on the Zn, Cu and MTI/II levels in the mouse brain. Brain Res 1013:134–141.

Chandrasekhar Y, Armstrong DT. 1989. Ability of progesterone to reverse anti-androgen (hydroxyflutamide)-induced interference with the preovulatory LH surge and ovulation in PMSG-primed immature rats. J Reprod Fertil 85:309–316.

Davis EC, Popper P, Gorski RA. 1996. The role of apoptosis in sexual differentiation of the rat sexually dimorphic nucleus of the preoptic area. Brain Res 734:10–18.

Diano S, Naftolin F, Horvath TL. 1997. Gonadal steroids target AMPA glutamate receptor-containing neurons in the rat hypothalamus, septum and amygdala: A morphological and biochemical study. Endocrinology 138:778–789.

Diano S, Naftolin F, Horvath TL. 1998. Kainate glutamate receptors (GluR5-7) in the rat arcuate nucleus: Relationship to tanycytes, astrocytes, neurons and gonadal steroid receptors. J Neuroendocrinol 10:239–247.

Dukes M, Furr BJ, Hughes LR, Tucker H, Woodburn JR. 2000. Nonsteroidal progestins and antiprogestins related to flutamide. Steroids 65:725–731.

Dunah AW, Hueske E, Wyszynski M, Hoogenraad CC, Jaworski J, Pak DT, Simonetta A, et al. 2005. LAR receptor protein tyrosine phosphatases in the development and maintenance of excitatory synapses. Nat Neurosci 8:458–467.

Gray LE Jr, Kelce WR. 1996. Latent effects of pesticides and toxic substances on sexual differentiation of rodents. Toxicol Ind Health 12:515–531.

Gu G, Varoqueaux F, Simerly RB. 1999. Hormonal regulation of glutamate receptor gene expression in the anteroventral periventricular nucleus of the hypothalamus. J Neurosci 19:3213–3222.

Han JS, Boeke JD. 2005. LINE-1 retrotransposons: Modulators of quantity and quality of mammalian gene expression? Bioessays 27:775–784.

Haoudi A, Semmes OJ, Mason JM, Cannon RE. 2004. Retrotransposition-competent human LINE-1 induces apoptosis in cancer cells with intact p53. J Biomed Biotechnol 2004:185–194.

Hardy DO, Niu EM, Catterall JF. 2001. Kap promoter analysis *in vivo*: A regulatory role for a truncated L1 repeat. Mol Cell Endocrinol 181:57–67.

Heiss NS, Bächner D, Salowsky R, Kolb A, Kioschis P, Poustka A. 2000. Gene structure and expression of the mouse dyskeratosis congenita gene, *dkc1*. Genomics 67: 153–163.

Hidalgo J, Aschner M, Zatta P, Vasak M. 2001. Roles of the metallothionein family of proteins in the central nervous system. Brain Res Bull 55:133–145.

Horie K, Urano T, Ikeda K, Inoue S. 2003. Estrogen-responsive RING finger protein controls breast cancer growth. J Steroid Biochem Mol Biol 85:101–104.

Ishitani K, Yoshida T, Kitagawa H, Ohta H, Nozawa S, Kato S. 2003. p54nrb acts as a transcriptional coactivator for activation function 1 of the human androgen receptor. Biochem Biophys Res Commun 306:660–665.

Kim D, Kim EH, Kim C, Sun W, Kim HJ, Uhm CS, Park SH, et al. 2003. Differential regulation of metallothionein-I, II, and III mRNA expression in the rat brain following kainic acid treatment. Neuroreport 14:679–682.

Kim HS, Shin JH, Moon HJ, Kim TS, Kang IH, Seok JH, Kim IY, et al. 2002. Evaluation of the 20-day pubertal female assay in Sprague-Dawley rats treated with DES, tamoxifen, testosterone, and flutamide. Toxicol Sci 67: 52–62.

Kocarek TA, Kraniak JM, Reddy AB. 1998. Regulation of rat hepatic cytochrome P450 expression by sterol biosynthesis inhibition: Inhibitors of squalene synthase are potent inducers of CYP2B expression in primary cultured rat hepatocytes and rat liver. Mol Pharmacol 54:474–484.

Koh DW, Dawson TM, Dawson VL. 2005. Poly(ADP-ribosyl)ation regulation of life and death in the nervous system. Cell Mol Life Sci 62:760–768.

Lund TD, Salyer DL, Fleming DE, Lephart ED. 2000. Pre or postnatal testosterone and flutamide effects on sexually dimorphic nuclei of the rat hypothalamus. Brain Res Dev Brain Res 120:261–266.

Maccioni RB, Cambiazo V. 1995. Role of microtubule-associated proteins in the control of microtubule assembly. Physiol Rev 75:835–864.

Marrone A, Walne A, Dokal I. 2005. Dyskeratosis congenita: Telomerase, telomeres and anticipation. Curr Opin Genet Dev 15:249–257.

Masutomi N, Shibutani M, Takagi H, Uneyama C, Takahashi N, Hirose M. 2003. Impact of dietary exposure to methoxychlor, genistein, or diisononyl phthalate during the perinatal period on the development of the rat endocrine/reproductive systems in later life. Toxicology 192: 149–170.

Matsumoto A, Sekine Y, Murakami S, Arai Y. 2000. Sexual differentiation of neuronal circuitry in the hypothalamus. In: Matsumoto A, editor. Sexual Differentiation of the Brain. Boca Raton: CRC Press, pp 203–227.

McCullough LD, Zeng Z, Blizzard KK, Debchoudhury I, Hurn PD. 2005. Ischemic nitric oxide and poly (ADP-ribose) polymerase-1 in cerebral ischemia: Male toxicity, female protection. J Cereb Blood Flow Metab 25:502–512.

McEwen BS, Alves SE. 1999. Estrogen actions in the central nervous system. Endocr Rev 20:279–307.

Meisel RL, Sachs BD. 1994. The physiology of male sexual behavior. In: Knobil E, Neills JD, editors. The Physiology of Reproduction, 2nd ed. New York: Raven Press, pp 3–106.

Meredith JM, Bennett C, Scallet AC. 2001. A practical three-dimensional reconstruction method to measure the volume of the sexually-dimorphic central nucleus of the medial preoptic area (MPOC) of the rat hypothalamus. J Neurosci Methods 104:113–121.

Mooney RA, LeVea CM. 2003. The leukocyte common antigen-related protein LAR: Candidate PTP for inhibitory targeting. Curr Top Med Chem 3:809–819.

Morales JF, Snow ET, Murnane JP. 2002. Environmental factors affecting transcription of the human L1 retrotransposon. I. Steroid hormone-like agents. Mutagenesis 17:193–200.

Morales JF, Snow ET, Murnane JP. 2003. Environmental factors affecting transcription of the human L1 retrotransposon. II. Stressors. Mutagenesis 18:151–158.

Muotri AR, Chu VT, Marchetto MC, Deng W, Moran JV, Gage FH. 2005. Somatic mosaicism in neuronal precursor cells mediated by L1 retrotransposition. Nature 435:903–910.

Nagao T, Saito Y, Usumi K, Kuwagata M, Imai K. 1999. Reproductive function in rats exposed neonatally to bisphenol A and estradiol benzoate. Reprod Toxicol 13:303–311.

Numan M. 1994. Maternal behavior. In: Knobil E, Neills JD, editors. The Physiology of Reproduction, 2nd ed. New York: Raven Press, pp 221–302.

Odum J, Lefevre PA, Tinwell H, Van Miller JP, Joiner RL, Chapin RE, Wallis NY, et al. 2002. Comparison of the developmental and reproductive toxicity of diethylstilbestrol administered to rats *in utero*, lactationally, preweaning, or postweaning. Toxicol Sci 68:147–163.

Orikasa C, Kondo Y, Hayashi S, McEwen BS, Sakuma Y. 2002. Sexually dimorphic expression of estrogen receptor β in the anteroventral periventricular nucleus of the rat preoptic area: Implication in luteinizing hormone surge. Proc Natl Acad Sci USA 99:3306–3311.

Orimo A, Inoue S, Ikeda K, Noji S, Muramatsu M. 1995. Molecular cloning, structure, and expression of mouse estrogen-responsive finger protein Efp. Co-localization with estrogen receptor mRNA in target organs. J Biol Chem 270:24406–24413.

Pieper AA, Blackshaw S, Clements EE, Brat DJ, Krug DK, White AJ, Pinto-Garcia P, et al. 2000. Poly(ADP-ribosyl) ation basally activated by DNA strand breaks reflects glutamate-nitric oxide neurotransmission. Proc Natl Acad Sci USA 97:1845–1850.

Preuss U, Bierbaum H, Buchenau P, Scheidtmann KH. 2003. DAP-like kinase, a member of the death-associated protein kinase family, associates with centrosomes, centromers, and the contractile ring during mitosis. Eur J Cell Biol 82:447–459.

Proteau A, Blier S, Albert AL, Lavoie SB, Traish AM, Vincent M. 2005. The multifunctional nuclear protein p54nrb is multiphosphorylated in mitosis and interacts with the mitotic regulator Pin1. J Mol Biol 346:1163–1172.

Reyna-Neyra A, Arias C, Ferrera P, Morimoto S, Camacho-Arroyo I. 2004. Changes in the content and distribution of microtubule associated protein 2 in the hippocampus of the rat during the estrous cycle. J Neurobiol 60:473–480.

Reyna-Neyra A, Camacho-Arroyo I, Ferrera P, Arias C. 2002. Estradiol and progesterone modify microtubule associated protein 2 content in the rat hippocampus. Brain Res Bull 58:607–612.

Rhees RW, Shryne JE, Gorski RA. 1990a. Onset of the hormone-sensitive perinatal period for sexual differentiation of the sexually dimorphic nucleus of the preoptic area in female rats. J Neurobiol 21:781–786.

Rhees RW, Shryne JE, Gorski RA. 1990b. Termination of the hormone-sensitive period for differentiation of the sexually dimorphic nucleus of the preoptic area in male and female rats. Dev Brain Res 52:17–23.

Rivas A, Fisher JS, McKinnell C, Atanassova N, Sharpe RM. 2002. Induction of reproductive tract developmental abnormalities in the male rat by lowering androgen production or action in combination with a low dose of diethylstilbestrol: Evidence for importance of the androgen-estrogen balance. Endocrinology 143:4797–4808.

Servomaa K, Rytomaa T. 1990. UV light and ionizing radiations cause programmed death of rat chloroleukaemia cells by inducing retropositions of a mobile DNA element (L1Rn). Int J Radiat Biol 57:331–343.

Sewer MB, Nguyen VQ, Huang CJ, Tucker PW, Kagawa N, Waterman MR. 2002. Transcriptional activation of human CYP17 in H295R adrenocortical cells depends on complex formation among p54nrb/NonO, protein-associated splicing factor, and SF-1, a complex that also participates in repression of transcription. Endocrinology 143:1280–1290.

Shibutani M, Masutomi N, Uneyama C, Abe N, Takagi H, Lee KY, Hirose M. 2005. Down-regulation of GAT-1 mRNA expression in the microdissected hypothalamic medial preoptic area of rat offspring exposed maternally to ethinylestradiol. Toxicology 208:35–48.

Shibutani M, Uneyama C. 2002. Methacarn: A fixation tool for multipurpose genetic analysis from paraffin-embedded tissues. In: Conn M, editor. Methods in Enzymology, Vol. 356. New York: Academic Press, pp 114–125.

Shibutani M, Uneyama C, Miyazaki K, Toyoda K, Hirose M. 2000. Methacarn fixation: A novel tool for analysis of gene expressions in paraffin-embedded tissue specimens. Lab Invest 80:199–208.

Shimada N, Suzuki T, Inoue S, Kato K, Imatani A, Sekine H, Ohara S, et al. 2004. Systemic distribution of estrogen-responsive finger protein (Efp) in human tissues. Mol Cell Endocrinol 218:147–153.

Skaper SD. 2003. Poly(ADP-ribose) polymerase-1 in acute neuronal death and inflammation: A strategy for neuroprotection. Ann NY Acad Sci 993:217–228; discussion 287–288.

Sogawa N, Sogawa CA, Oda N, Fujioka T, Onodera K, Furuta H. 2001. The effects of ovariectomy and female sex hormones on hepatic metallothionein-I gene expression after injection of cadmium chloride in mice. Pharmacol Res 44:53–57.

Suzuki K, Nakajima K, Otaki N, Kimura M. 1994. Metallothionein in developing human brain. Biol Signals 3:188–192.

Takagi H, Shibutani M, Kato N, Fujita H, Lee KY, Takigami S, Mitsumori K, et al. 2004. Microdissected region-specific gene expression analysis with methacarn-fixed, paraffin-embedded tissues by real-time RT-PCR. J Histochem Cytochem 52:903–913.

Tena-Sempere M, Gonzalez LC, Pinilla L, Huhtaniemi I, Aguilar E. 2001. Neonatal imprinting and regulation of estrogen receptor α and β mRNA expression by estrogen in the pituitary and hypothalamus of the male rat. Neuroendocrinology 73:12–25.

Thornton JE, Irving S, Goy RW. 1991. Effects of prenatal antiandrogen treatment on masculinization and defeminization of Guinea pigs. Physiol Behav 50: 471–475.